BBA - Gene Regulatory Mechanisms 1867 (2024) 195064

Contents lists available at ScienceDirect

BBA - Gene Regulatory Mechanisms

journal homepage: www.elsevier.com/locate/bbagrm

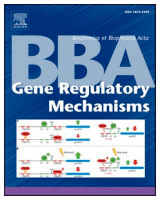

Research paper

EBV infection alters DNA methylation in primary human colon cells: A path to inflammation and carcinogenesis?

Roberta Santarelli [a,*,1], Giuseppe Rubens Pascucci [b,c,1], Salvatore Lo Presti [a], Michele Di Crosta [a], Rossella Benedetti [a], Alessia Neri [b,c], Roberta Gonnella [a], Mara Cirone [a,*]

[a] Department of Experimental Medicine, "Sapienza" University of Rome, 00161 Rome, Italy
[b] Research Unit of Clinical Immunology and Vaccinology, Bambino Gesù Children's Hospital, Istituto di Ricovero e Cura a Carattere Scientifico (IRCCS), Rome, Italy
[c] Department of Systems Medicine, University of Rome "Tor Vergata", Rome, Italy

ARTICLE INFO

Keywords:
EBV
IBD
Carcinogenesis
Epigenetic
Methylation
ERK1/2
STAT3
PAA

ABSTRACT

Epstein-Barr Virus (EBV) is associated with several types of human cancers, and changes in DNA methylation are reported to contribute to viral-driven carcinogenesis, particularly in cancers of epithelial origin. In a previous study, we demonstrated that EBV infects human primary colonic cells (HCoEpC) and replicates within these cells, leading to pro-inflammatory and pro-tumorigenic effects. Notably, these effects were mostly prevented by inhibiting viral replication with PAA. Interestingly, the EBV-induced effects correlated with the upregulation of DNMT1 and were counteracted by pretreating cells with 5-AZA, suggesting a role for DNA hypermethylation.

Building on this background, the current study investigates the methylation changes induced by EBV infection in HCoEpC, both in the presence and absence of PAA, or ERK1/2 and STAT3 inhibitors, pathways known to be activated by EBV and involved in the dysregulation of methylation in tumor cells. The genome-wide methylation analysis conducted in this study allowed us to identify several biological processes and genes affected by these epigenetic changes, providing insights into the possible underlying mechanisms leading to the pathological effects induced by EBV. Specifically, we found that the virus induced significant methylation changes, with hypermethylation being more prevalent than hypomethylation. Several genes involved in embryogenesis, carcinogenesis, and inflammation were affected.

1. Introduction

EBV was the first human oncovirus to be discovered in 1964, and the number of cancers associated with the virus has been increasing over time. EBV is linked to several types of B-cell lymphomas and epithelial cancers, such as nasopharyngeal carcinoma (NPC) and a subset of gastric cancers (GC) [1]. Moreover, the virus has been detected in the most severe forms of inflammatory bowel disease (IBD) [2,3], pathologic conditions that may predispose to the onset of colon cancer [4]. Indeed, chronic inflammation is known to increase the risk of cancer, also by inducing an aberrant DNA methylation, as reported in the case of gastric cancer related to *Helicobacter pylori* and EBV [5]. However, the involvement of EBV in colon carcinogenesis, suggested by previous studies [6–8], remains a controversial issue.

Epigenetic modifications, particularly DNA hypermethylation, are among the mechanisms through which EBV restricts viral antigen expression to establish latency and dysregulates host gene expression in its-associated cancer cells, particularly those of epithelial origin [9,10].

DNA hypermethylation is mediated by DNA methyltransferases (DNMTs), enzymes that transfer a methyl group to cytosine at position 5 to form 5-methylcytosine (5mC), process that in mammals mainly occurs in the CG dinucleotide context (CpG). About 70 % to 80 % of CpG sites, distributed across the entire genome, are methylated, mainly to silence the transposable and viral elements, which represent approximately 45 % of the human genome. An exception is represented by the CpG islands, regions with a high CpG density, in which about 70 % of promoters reside, whose methylation level is lower compared to the rest of the genome [11]. 5mC controls gene expression as it recruits proteins involved in gene repression or inhibits the binding to DNA of transcription factors [11,12]. While physiological DNA methylation regulates tissue-specific gene expression, genomic imprinting and X chromosome inactivation [11], the aberrant DNA methylation

* Corresponding authors.
E-mail addresses: roberta.santarelli@uniroma1.it (R. Santarelli), mara.cirone@uniroma1.it (M. Cirone).
[1] Equally contributed to the study

https://doi.org/10.1016/j.bbagrm.2024.195064
Received 10 June 2024; Received in revised form 2 October 2024; Accepted 14 October 2024
Available online 18 October 2024

contributes to the onset of human diseases, including inflammatory diseases such as IBD [13], in which DNA methylation changes are enriched in inflammation-related pathways [14] and cancer, in which these changes lead to a reduced expression of tumor suppressor genes or an upregulation of that of oncogenes [15].

Changes in DNA methylation has been shown to be exploited by the most of human oncoviruses as a common mechanism to promote chronic inflammation, genome instability, increased cell proliferation and to escape from apoptosis, among other pro-tumorigenic effects [16].

Regarding EBV, we have recently reported that the virus infected human primary colonic cells (HCoEpC) and that, after 72 h of infection, it replicated in these cells, promoting pro-inflammatory cytokine secretion and other pro-tumorigenic effects such as autophagy and DNA damage response (DDR) dysregulation. These effects occurred in correlation with DNMT1 upregulation and were counteracted by the DNA-demethylating agent 5-azacytidine (5-AZA) [17]. Based on these findings and on the evidences previously reported that EBV may hijack host epigenetic machinery to drive tumorigenesis [10], in the present study we performed a genome-wide DNA methylation analysis and investigated the methylation changes induced by the virus in HCoEpC. HCoEpC model enables the identification of the genes epigenetically modified by EBV-infection, which could contribute to the pro-inflammatory and pro-tumorigenic effects induced by it at the early stages of infection in epithelial cells. This cannot be done in virus-associated tumor cells, as the epigenetic changes observed in cancer cells may not reflect those that occur in the early stages of infection, when EBV-driven inflammatory and/or oncogenic processes may begin. As we have previously shown that EBV replicated in HCoEpC after 72 h of infection, and that phosphonoacetic acid (PAA) prevented DNMT1 upregulation as well as most of the pro-tumorigenic effects induced by the virus [17], here we also evaluated the impact of PAA pretreatment on the methylation changes in infected HCoEpC cells. Finally, the role of ERK1/2 and STAT3 was assessed, as the first was found to be activated by EBV-infection in HCoEpC [17] and as both pathways have been shown to contribute to dysregulate methylation in virus-associated cancer cells [9]. The biological processes and molecular functions related to the regions whose methylation was altered by EBV as well as the genes hypermethylated or hypomethylated by the virus, in the presence or in the absence of PAA or PD0325901 and AG490 (ERK1/2 and STAT3 inhibitors, respectively), were analyzed in an attempt to shed light on epigenetic changes and the molecular mechanisms that regulate them during the initial stages of EBV infection, when the virus could trigger inflammation and initiate the transformation of epithelial cells.

2. Materials and methods

2.1. Cell cultures

Primary human colonic epithelial cells (HCoEpC; iXCells Biotechnologies) were cultured in Epithelial Cell Growth Medium (iXCells Biotechnologies, Cat# MD-0041). Prior infection or treatments, 5×10^4 HCoEpC were seeded /well in 6-well plates and grown up to 80 % confluency.

B95–8 is an EBV positive marmoset cell line, that was cultured in RPMI 1640 (Sigma-Aldrich, St Louis, MO, USA, R0883), 10 % fetal bovine serum (FBS; SigmaAldrich, F7524), 2 mM glutamine (Aurogene, Rome, Italy, AU-X0550), 100 mg/ml streptomycin and 100 U/ml penicillin (Aurogene, AUL0022), in 5 % CO2-saturated humidity at 37 °C.

2.2. EBV isolation

B95–8 cells were treated with 12- O-tetradecanoylforbol-13-acetate (TPA, 30 ng/ml, Sigma-Aldrich; P8139) and Sodium-butyrate (3 mM, Sigma-Aldrich; B5887) for 96 h to activate EBV lytic cycle and, consequently, allow virus production. Then, the cells were centrifuged at 1500 rpm for 5 min at 4 °C and the supernatant containing EBV was filtered through 0.45 μm pore-size filters. Next, virus particles were harvested by ultracentrifugation at 29.000 rpm for 90 min at 4 °C, resuspended in Epithelial Cell Growth, aliquoted (10^7 EBV DNA copies/50 μl) and stored at −80 °C.

2.3. HCoEpC infection

As previously described, 5×10^4 HCoEpC were exposed to 10^7 EBV DNA copies and, after one hour incubation at 37 °C, they were spinoculated at 1400 rpm for 1 h at 37 °C. Uninfected cells were used as control. Subsequently, the supernatant was replaced with fresh Epithelial Cell Growth Medium and the cells were grown at 37 °C for additional 72 h. Next, ELITE MGB kit (ELITech) was used to evaluate HCoEpC infection [17].

2.4. Reagents and treatments

PD0325901 (1 μM, PD, MedChemExpress, HY-10,254) and AG490 (20 μM, AG, Millipore #658411) were used to inhibit ERK1/2 and STAT3, respectively. Moreover, Phosphonoacetic acid (500 μM, PAA, Sigma-Aldrich, #284,270) was used as an EBV DNA replication and late gene expression inhibitor. 5-Azacytidine (5-AZA) (0.5 μM) was used as de-methylating agent. HCoEpC were preincubated with the appropriate inhibitors for 45 min and then infected with EBV.

DMSO was used as a vehicle and uninfected HCoEpC were used as control.

2.5. Genomic DNA purification

Genomic DNA was purified with PureLink genomic DNA mini kit (Invitrogen, #K182001) from 10^6 EBV-infected and uninfected HCoEpC, pretreated or not with PAA or PD/AG, and then quantified by Nanodrop.

2.6. Oxford Nanopore Technologies (ONT) library preparation and sequencing

Genomic DNA was sheared to ~6 kb fragment size using Covaris G tubes and DNA concentration was assessed using the dsDNA BR assay on a Qubit fluorometer (Thermo Fisher). Nanopore sequencing libraries were prepared using the native library prep kit SQK-LSK110 according to the manufacturer's instructions. The library of each sample was loaded into an R9.4.1 MinION flow cell (FLO-MIN106) and sequenced on an ONT MinION device with MinKNOW acquisition software version v.22.10.10. The samples were run for a maximum duration of 72 h.

2.7. Methylation calling

Raw sequencing data were basecalled with the standalone Guppy basecaller (v.6.4.6) using the high accuracy model "dna_r9.4.1_450bps_modbases_5mc_cg_hac.cfg" that also calls 5'methycytosine in the CpG context. The reads with a q score < 7 were discarded. Specifying the reference genome sequence (Gencode hg38) with the –align_ref parameter, Guppy generates mapped or unmapped bam files. The bam files were then converted to bed format with modbam2bed 0.7.0 aggregating the methylation levels between the strands.

2.8. Differential methylation analysis

CpG sites with read depths <4 or >50 were discarded from further analyses. The MethylKit R package was used to perform pairwise comparisons of methylation levels. Samples of interest were merged into one object containing common CpGs. Using the normalizeCoverage function, the median method was used to normalize the methylation matrix. Differentially Methylated Regions (DMRs) were defined as regions with a methylation difference >20 % and an *p*-value adjusted by False Discovery Rate (FDR)-adjusted p-value <0.05 over 250 bp tiling windows

with a step of 250 bp. Annotation of DMRs was done by using the annotatePeaks.pl function of the Homer tool (v.4.11) [18]. To obtain the Differentially Methylated Genes (DMGs) we calculated the mean methylation difference values of the Differentially Methylated Regions (DMRs) for each gene. Then we considered only genes with a methylation difference value >20 or less than −20. All statistical analyses of methylation levels were performed with R version 4.1.1 R Core Team (2021) [19].

2.9. Functional analysis

To investigate the biological processes and molecular functions DMRs were involved in, we performed a functional analysis using the Genomic Regions Enrichment of Annotations Tool (GREAT) R package (v 2.0.2) [20] with the following parameters: rule = "oneClosest", adv_oneDistance = 1000. Only terms with an FDR-adjusted *p*-value <0.05 were considered statistically significant. We further investigated the motifs of DNA binding proteins associated with the differentially methylated regions using the findMotifsGenome.pl function with the "size given" parameter of the Homer tool [18].

RNA isolation, reverse transcription and quantitative real time polymerase chain reaction (RT-qPCR).

RNA was extracted from EBV-infected and uninfected control HCoEpC, treated or not with PAA or PD/AG, by using TRIzol™ Reagent (Life Technologies Corporation, Carlsbad, CA, USA, 15,596,026) according to the manufacturer's instructions, and then incubated with RNase-free DNase I (Norgen Biotek Corp.) for 10 min at RT. Next, RT-qPCR analyses were carried out to evaluate the expression of BZLF1 and gp220 EBV lytic genes and of HOXB4 and WNT11 as well. To this purpose, reverse transcription was performed with High-Capacity Reverse Transcription kit (Applied Biosystems, 4,368,814) and Real Time-PCR with SensiFast SYBR No-ROX kit (Bioline). As a further control, RT-qPCR was carried out in the absence of reverse-transcriptase (data not shown). Beta-actin was used as reference gene and $2 - \Delta\Delta Ct$ method was used to normalize gene transcription data.

Primers used were:
BZLF1 Fw-5′-TCGCATTCCTCCAGCGATT-3′.
BZLF1 Rv-5′-CAAGGACAACAGCTAGCAGACATT-3′.
gp220 Fw-5′-CCTGTGTTATATTTTCACCACTTTC-3′.
gp220 Rv-5′-ACCGCACCTGCAAGCA-3′.
HOXB4 Fw-5′-TTCTGACATTCCAAAACCAG-3′.
HOXB4 Rv-5′-TTGCTGGTCACAAGAAAC-3′.
WNT11 Fw-5′-ACTAGCTTGGGTTGTAAATG-3′.
WNT11 Rv-5′-ACCCCAAAGAAAAAGCTATG-3′.
Actin Fw-5′-TCATGAAGTGTGACGTGGACATC-3′.
Actin Rv-5′-CAGGAGGAGCAATGATCTTGATCT-3′.

2.10. Western blotting

To extract proteins, cells were lysed in RIPA buffer (NaCl 150 mM, NP40 1 %, Tris–HCl pH 8 50 mM, deoxycholic acid 0.5 %, SDS 0.1 %) containing protease and phosphatase inhibitors. Then, 10 μg of protein extract were loaded on a precast polyacrylamide gel (Bolt™ 4–12 % Bis-Tris Plus, Invitrogen, Waltham, MA, USA) and subsequently transferred to a nitrocellulose membrane (Amersham ™). After 30 min in blocking solution (PBS, 0.1 % Tween 20, 2 % BSA), membranes were incubated with primary antibody 1 h at room temperature or overnight at 4 °C, washed thrice in PBS-0.1 % Tween 20 (washing solution) and then incubated for 30 min with a secondary antibody conjugated to horseradish peroxidase (HRP). Next, membranes were washed thrice with washing solution and protein detection was performed through a chemiluminescence kit Western Bright ECL (Advansta, Menio Park, CA, USA). Finally, a densitometric analysis was carried out using ImageJ software.

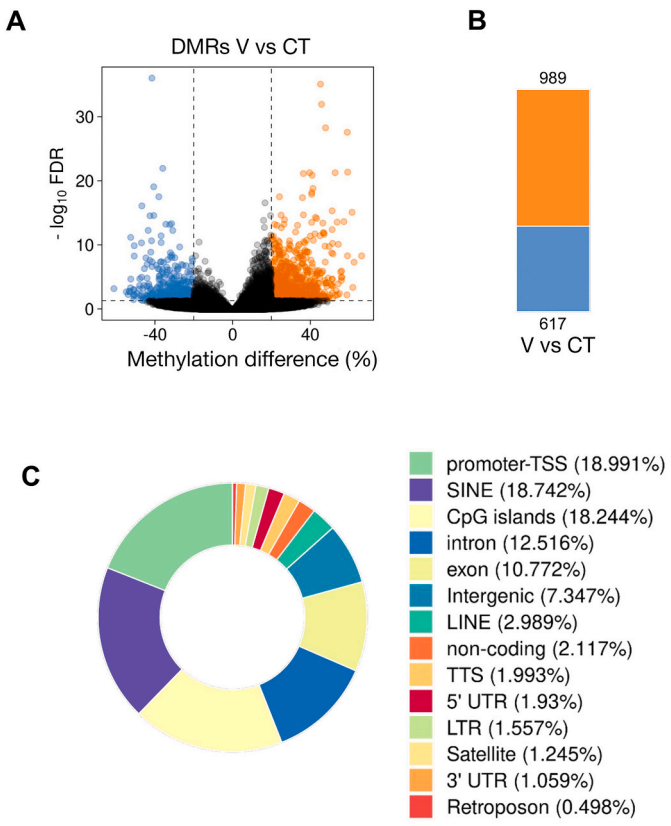

Fig. 1. Changes in the whole genome DNA methylation in HCoEpC following EBV infection. (A) Volcano plot showing the results of differential methylation analysis between EBV-infected (V) and uninfected control HCoEpC (CT). Each point in the plot represents a genomic region, with the x-axis indicating the percentage of methylation difference, and the y-axis representing the negative log10 of the FDR-adjusted *p*-value. The orange dots represent regions that are significantly hypermethylated after EBV infection, with a methylation difference >20 % and an adjusted p-value <0.05. Blue dots depict regions significantly hypomethylated after EBV infection, with a methylation difference less than −20 % and an adjusted p-value <0.05. The dashed lines represent significance thresholds (methylation difference = ±20 %, FDR adjusted p-value = 0.05). (B) Number of significantly hypermethylated (orange) and hypomethylated (blue) regions after EBV infection. (C) Pie chart indicating the genomic location of DMRs found following EBV infection.

2.11. Antibodies

The following antibodies were used: mouse monoclonal anti-phospho ERK1/2 (1:500) (Santa Cruz Biotechnology Inc., Biotechnology Inc., Cat# sc-7383, Dallas, TX, USA); rabbit polyclonal anti-ERK1 and anti-ERK2 (1:500) (Santa Cruz Biotechnology Inc., Biotechnology Inc., Cat# sc193 and Cat# sc-154, Dallas, TX, USA); mouse monoclonal anti-phospho STAT3 (1:500) (pY705, BD Biosciences, Cat# 612356), mouse monoclonal anti-STAT3 (1:500) (BD Biosciences, Cat# 6101289); mouse monoclonal anti-β Actin (1:10.000) (Sigma Aldrich, Cat# A5441, Burlington, MA, USA). Goat polyclonal anti-mouse HRP-conjugated (Santa Cruz Biotechnology Inc., Cat# sc-2005, Dallas, TX, USA) and anti-rabbit HRP-conjugated (1:15.000) (Santa Cruz Biotechnology Inc., Cat# sc-2004, Dallas, TX, USA) were used as secondary antibodies.

2.12. Densitometric analysis

The Image J software (1.47 version, NIH, Bethesda, MD, USA), downloaded from the NIH website (http://imagej.nih gov, accessed on 10 February 2022), was used for densitometric analysis of protein bands.

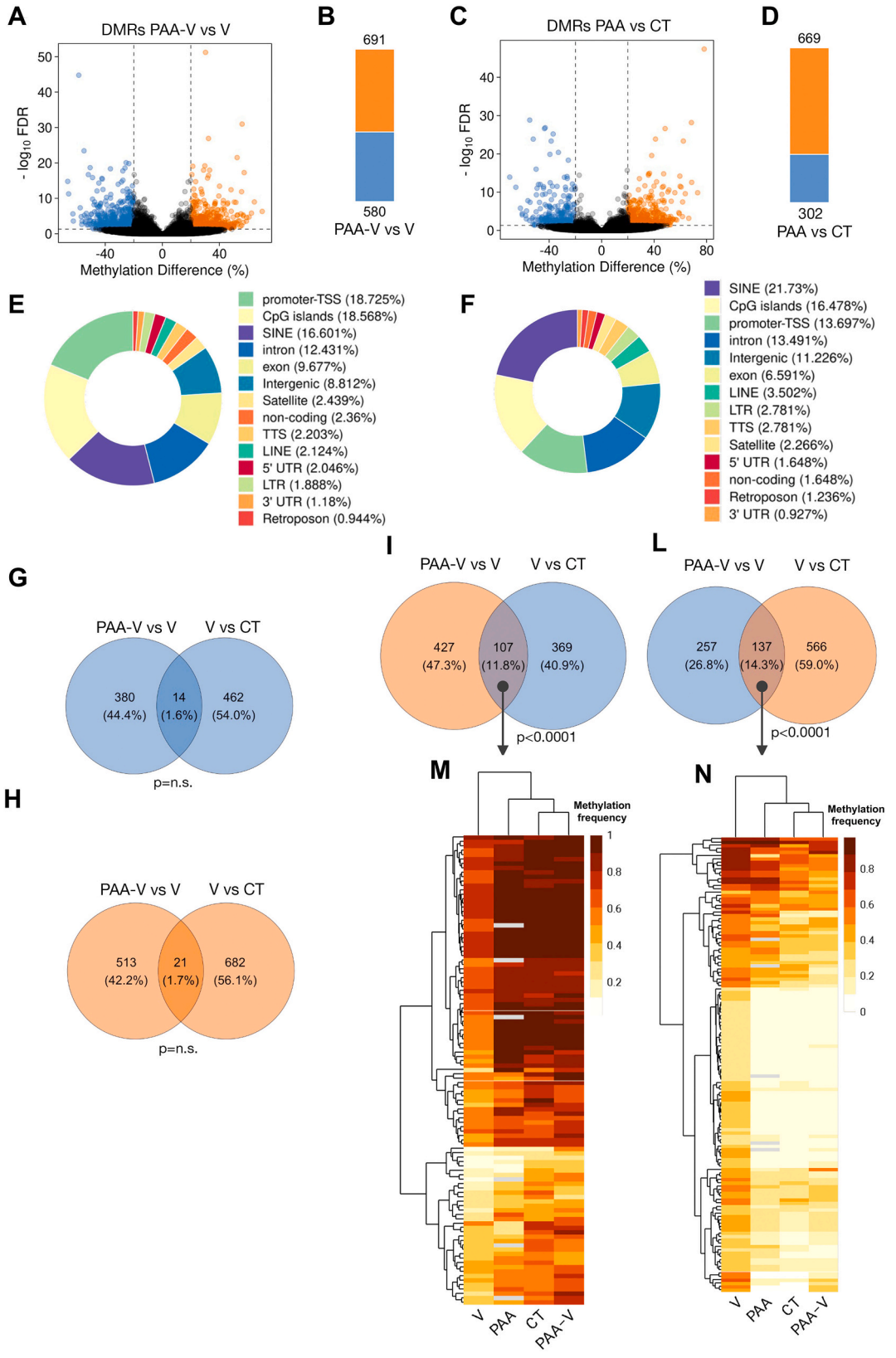

(caption on next page)

Fig. 2. Effect of PAA pretreatment on EBV-induced methylation changes. (A) Volcano plots depicting the differential methylation analysis of EBV-infected HCoEpC pretreated with PAA (PAA-V) versus EBV-infected cells (V). The orange dots represent genomic regions that are significantly hypermethylated, while the blue ones indicate regions significantly hypomethylated and the dashed lines represent significance thresholds (methylation difference = + / -20 %, FDR adjusted p-value = 0.05). (B) Number of significantly hypermethylated (orange) and hypomethylated (blue) regions in PAA-V vs. V. (C) Volcano plots showing the differential methylation analysis of HCoEpC treated with PAA (PAA) compared to uninfected control HCoEpC (CT). The orange dots represent regions that are significantly hypermethylated while the blue ones the regions significantly hypomethylated and the dashed lines the significance thresholds (methylation difference = + / -20 %, FDR adjusted p-value = 0.05); (D) Number of significantly hypermethylated (orange) and hypomethylated (blue) regions in PAA vs. CT.
Pie charts that indicate the genomic localisation of DMRs found (E) in EBV-infected pretreated with PAA (PAA-V) versus EBV-infected HCoEpC (V), and (F) in cells treated with PAA vs. uninfected control HCoEpC.
Venn diagrams showing the intersections of hypomethylated (G) and hypermethylated (H) genes of EBV-infected HCoEpC pretreated with PAA versus EBV-infected cells (PAA-V vs. V) and EBV-infected cells versus uninfected control HCoEpC (V vs. CT). Each DMR was associated to the nearest genegGenes using the Homer tool. The methylation mean of all DMRs related each gene was calculated and only genes that still had a methylation difference >20 % were considered. *p* values were calculated by using Chi-squared test. (I) Intersection of genes hypomethylated following EBV infection (V vs. CT) and hypermethylated in EBV-infected HCoEpC pretreated with PAA (PAA-V vs. V). (L) Intersection of genes hypermethylated after EBV infection (V vs. CT) and hypomethylated by pretreatment with PAA prior infection (PAA-V vs. V).
Heatmap showing the methylation frequency of (M) the 107 genes hypomethylated after EBV infection (V vs. CT) and hypermethylated after infection following pretreatment with PAA (PAA-V vs. V) and (N) of the 137 genes hypermethylated after EBV infection (V vs. CT) and hypomethylated by pretreatment with PAA prior infection (PAA-V vs. V). The color intensity is proportional to the methylation frequency: lighter colors indicate a low methylation level and vice versa. Grey cells indicate values that are not available.

2.13. Statistical analysis

Results are shown as the mean ± standard deviation (SD) of three independent experiments. Statistical analysis was performed by Student's *t*-test. Difference was considered as statistically significant when *p*-value was <0.05 and indicated with * in the figures, while p-value ≥0.05 was considered not significant and not indicated in the figures.

3. Results

3.1. EBV infection changes genome methylation in HCoEpC

We have previously reported that EBV infected HCoEpC and that, after 72 h of infection, it induced several pro-inflammatory and pro-tumorigenic effects, including autophagy and DDR dysregulation, in correlation with DNMT1 up-regulation. As 5-AZA prevented most of these effects, in the present study, we explored, at the same time post-infection, the whole genome methylation of EBV-infected (V) and uninfected control (CT) HCoEpC by using third-generation sequencing technology from Oxford Nanopore Technologies (ONT). After filtering by read quality and site coverage, the level of methylation was evaluated in approximately 19 million CpG sites in both V and CT samples.

The methylation changes induced by EBV-infection in HCoEpC were evaluated by comparing a sliding window of 250 bp between the infected and control cells and using the methylkit R package. We considered as Differential Methylated Regions (DMRs), those with a methylation difference >20 % and an FDR adjusted *p*-value <0.05 (Fig. 1A). By comparing virus-infected and uninfected control HCoEpC, we found that 1606 regions showed significant methylation changes (Fig. 1B), and that among those, 989 regions were hypermethylated and 617 were hypomethylated (Fig. 1B), suggesting that EBV infection was mainly driving hypermethylation. We then observed that the three most frequent localizations of DMRs were promoters (19 %), SINE (18.7 %) and CpG islands (18.2 %) (Fig. 1C).

3.2. Several methylation changes induced by EBV-infection are prevented by PAA-pretreatment

We have previously found that pretreatment by PAA, a drug able to inhibit viral DNA synthesis and late lytic protein expression [21], prevented the up-regulation of DNMT1 as well as most of the pro-inflammatory and pro-tumorigenic effects induced by EBV infection in HCoEpC. We therefore evaluated methylation changes induced by EBV in the presence or in the absence of PAA. After confirming that cells were EBV-infected, as they expressed ZEBRA and gp220 after 72 h and that PAA pretreatment was able to prevent the expression of the late lytic gene gp220 in HCoEpC (Supp. Fig. S1A and S1B) without affecting cell survival (Supplementary Fig. S2A), we found 1271 DMRs between EBV-infected cells pretreated with PAA versus those untreated (PAA-V vs V) (Fig. 2A), of which 691 were hypermethylated and 580 hypomethylated (Fig. 2B). PAA induced some methylation changes also in the uninfected control cells (Fig. 2C and D), although it affected different regions compared to the infected cells (Fig. 2E and F). Next, to evaluate whether PAA pretreatment could prevent methylation of the genes hyper- or hypo-methylated by EBV in infected HCoEpC, we investigated the methylation changes at gene-level. To this end, we aggregated by average the methylation difference of the regions associated with each gene and then filtered only genes that still had a methylation difference higher than 20 %. Venn diagrams shown in Fig. 2G and H, suggest that few genes were methylated in the same direction in virus-infected cells versus control (V vs CT) compared to PAA-treated infected cells versus the untreated infected cells (PAA-V vs V), being only 1,6 % hypo-methylated and 1,7 % hypermethylated, in both comparisons. Conversely, we found a higher proportion of common genes (107, = 11.8 %) when we intersected genes hypomethylated in EBV-infected (V vs CT) with those hypermethylated in PAA-treated infected cells (PAA-V vs V) (Fig. 2I). Also, the intersection of genes hypermethylated in EBV-infected HCoEpC (V vs CT) compared to those hypomethylated in PAA-treated infected cells (PAA-V vs V) showed a higher proportion of common genes (137, = 14.3 %) (Fig. 2L). The heatmaps in Fig. 2M and N recapitulate the levels of hypomethylation (lighter color) and the hypermethylation (darker color) of these genes. All together these results suggest that PAA could prevent several methylation changes induced by EBV infection in HCoEpC.

3.3. ERK1/2 and STAT3 activation contributes to the methylation changes induced by EBV

In our previous study, we showed that ERK1/2 inhibition was involved in several pro-tumorigenic effects induced by EBV in HCoEpC [17]. After confirming that the virus activated ERK1/2 in these cells (Fig. 3A), we investigated if viral infection could activate also STAT3, a pathway known to be strongly involved in EBV-driven carcinogenesis [22,23] and to contribute to alter methylation in other cell types [9]. Here, we observed that STAT3 and ERK1/2 were concomitantly activated by EBV infection in HCoEpC (Fig. 3B). Their inhibition by PD0325901 and by AG490 in combination (PD/AG), that slightly affected cell survival (Supplementary Fig. S2B), downregulated DNMT1 expression level (Fig. 3C). while the single treatment by PD or AG slightly affected it (Supplementary Fig. S3) We then investigated whether the inhibition of both pathways could prevent the methylation changes induced by the virus in these cells. We found that 1015 regions were differentially methylated in EBV-infected cells pretreated with PD/AG (PD/AG-V) versus those untreated (V) and, among them, 515 regions

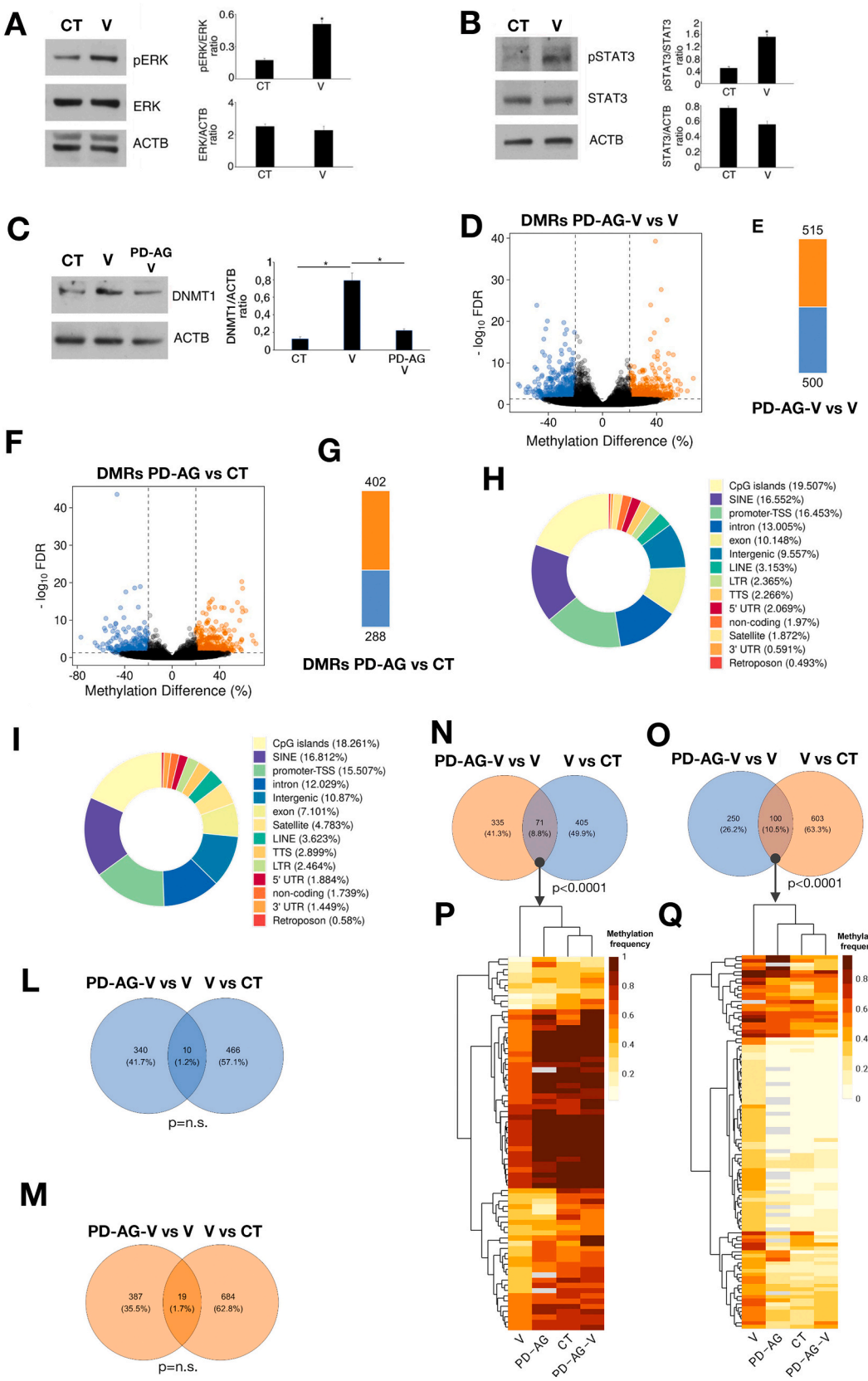

(caption on next page)

Fig. 3. Effect of pretreatment with PD/AG on methylation changes induced by EBV. Western blot analysis showing the activation of (A) ERK1/2 (pERK) and (B) STAT3 (pSTAT3) in EBV-infected (V) and control (CT) HCoEpC, at 72 h p.i. (C) Western blot analysis showing DNMT1 expression in infected cells pretreated or nor with PD/AG. One representative experiment is shown. Beta-actin (ACTB) was used as loading control and histograms represent the mean plus SD of the densitometric analysis of the ratio of pERK/ERK, ERK/ACTB, pSTAT3/STAT3, STAT3/ACTB and DNMT1/ACTB of three different experiments. (D) Volcano plots depicting the results of the differential methylation analysis between EBV-infected cells pretreated with PD/AG (PD-AG-V) vs. EBV-infected cells (V) (E) Number of regions significantly hypermethylated (orange) and hypomethylated (blue) in PD-AG-V vs. V. (F) Volcano plots showing the results of the differential methylation analysis between HCoEpC treated with PD/AG (PD-AG) and control HCoEpC (CT). (G) Number of regions significantly hypermethylated (orange) and hypomethylated (blue) in PD-AG vs. CT. In both the Volcano plots, the orange dots represent regions that are significantly hypermethylated while the blue ones indicate the regions significantly hypomethylated, and the dashed lines represent significance thresholds (methylation difference = + / -20 %, FDR adjusted p value = 0.05). Pie charts indicate the genomic localisation of DMRs found (H) between EBV-infected cells pretreated with PD/AG (PD-AG-V) and EBV-infected cells (V) or (I) between HCoEpC treated with PD/AG (PD-AG) and control (CT) HCoEpC.
Venn diagram showing the intersections of genes hypomethylated (L) and hypermethylated (M) of EBV-infected HCoEpC pretreated with PD/AG versus EBV-infected cells (PD-AG-V) and EBV-infected HCoEpC vs uninfected control cells (V vs. CT). p values were calculated by using Chi-squared test. Genes were associated with DMRs using the Homer tool. The methylation mean of all DMRs associated with each gene was calculated and only genes that still had a methylation difference >20 % were considered. Intersection of genes (N) hypomethylated following EBV infection (V vs. CT) and hypermethylated by the pretreatment with PD/AG (PD-AG-V vs. V) or (O) hypermethylated after EBV infection (V vs. CT) and hypomethylated by pretreatment with PD/AG (PD-AG-V vs. V).
Heatmaps showing the frequency of methylation (P) of the 71 genes hypomethylated after EBV infection (V vs CT) and hypermethylated by pretreatment with PD/AG (PD-AG-V vs V) and (Q) of the 100 genes hypermethylated after EBV infection (V vs. CT) and hypomethylated by pretreatment with PD/AG (PD-AG-V vs. V). The color intensity is proportional to the methylation frequency: lighter colors indicate a low methylation level and vice versa. Grey cells indicate values that are not available.

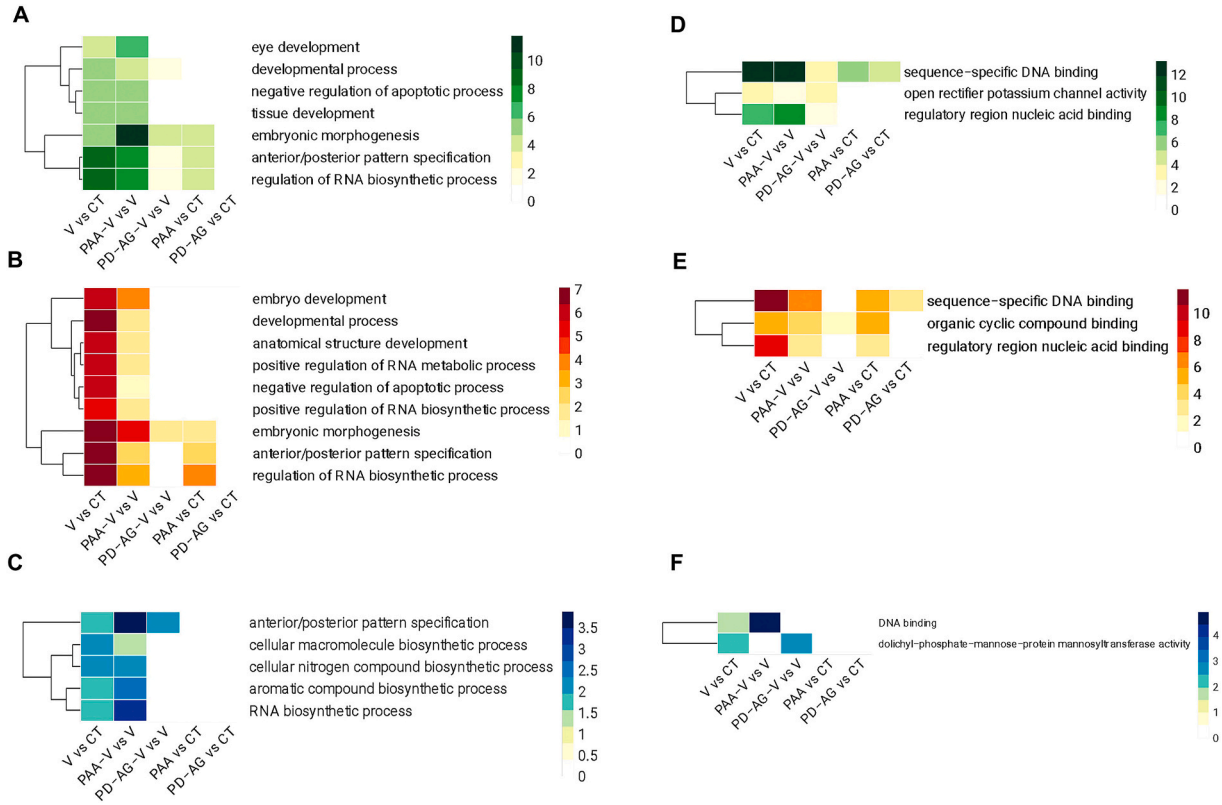

Fig. 4. Functional analysis of the DMRs. Heatmaps showing the significance levels as -log (FDR-adjusted *p*-value) of the functional analysis on biological processes (A, B C) and molecular functions (D, E, F) performed using the Genomic Regions Enrichment of Annotations Tool (GREAT). The different heatmaps in the figure are displayed in different colors: a green color scale for all the DMRs (A, D), a blue color scale for the hypomethylated regions (B, E), and a red color scale for the hypermethylated regions (C, F). Darker colors are proportional to more significant enrichment results, while not significant terms (FDR-adjusted p-value > ≤ 0.05) are shown in white.

were hypermethylated and 500 hypomethylated (Fig. 3D and E). PD/AG also induced some changes in methylation in several regions in uninfected control cells (CT) (Fig. 3F and G). The DMRs were mainly located within the CpG islands, SINE and promoters, with similar proportions in both comparisons (Fig. 3H and I). As shown in Venn diagrams reported in Fig. 3L and M, EBV-infected cells pretreated with PD/AG versus untreated infected cells (PD-AG-V vs. V) and EBV-infected versus control cells (V vs. CT) shared a small proportion of common hypomethylated (1,2 %) and hypermethylated (1,7 %) genes. The intersections of genes hypomethylated by EBV and hypermethylated by PD/AG (Fig. 3N) and vice versa (Fig. 3O) showed a higher proportion of common genes, which were 71 (8.8 %) and 100 (10.5 %) genes, respectively. The heatmaps in Fig. 3P and Q show the hypomethylation (lighter color) and hypermethylation (darker color) levels of the common genes. These results suggest that some of the EBV-induced methylation changes in HCoEpC could be prevented by PD/AG pretreatment.

EBV differently methylates genes regulating embryonic development, RNA biosynthetic and developmental processes, and apoptosis, effect prevented by PAA and, to a lesser extent, by PD/AG.

We next investigated which biological processes and molecular

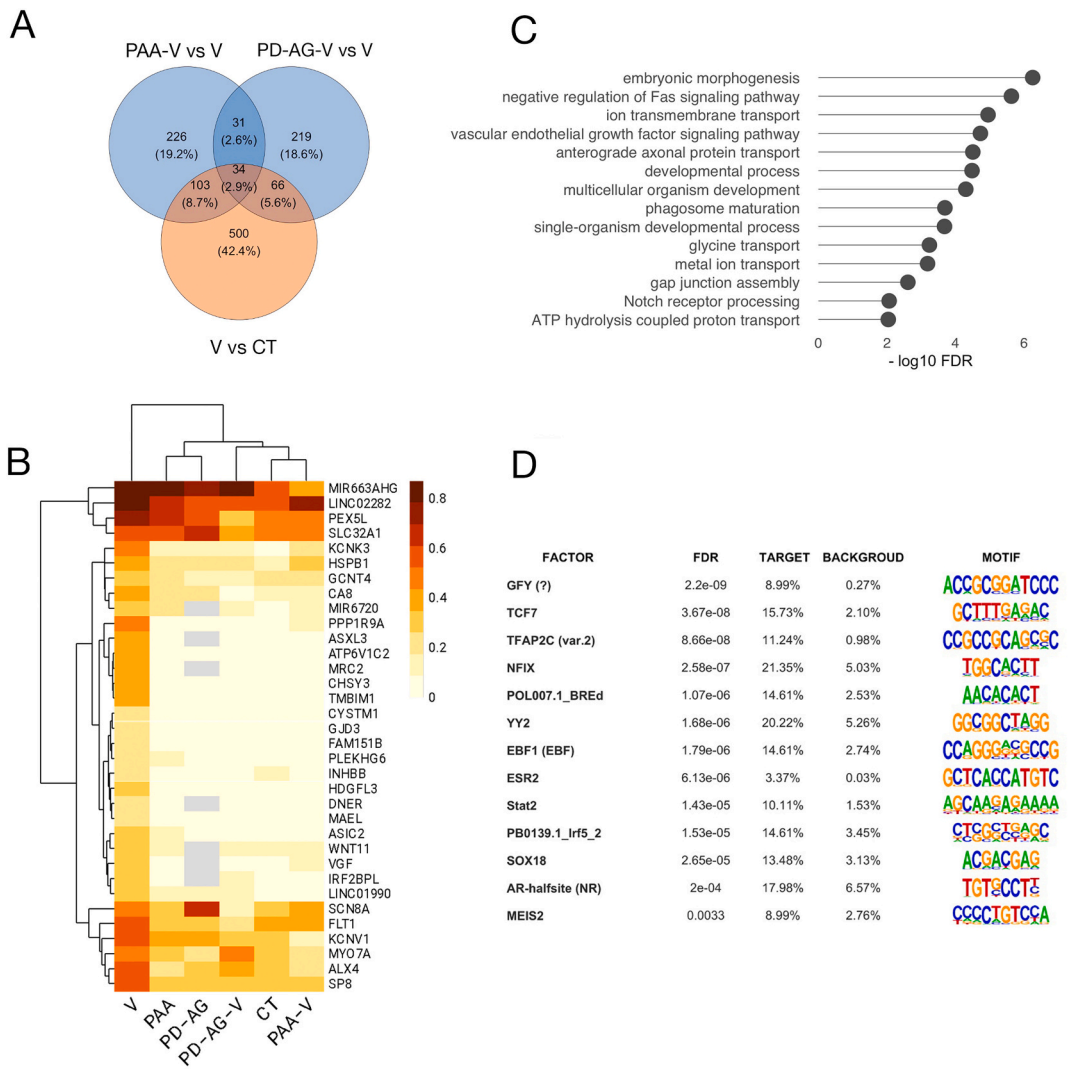

Fig. 5. Genes hypermethylated by EBV and hypomethylated by PAA or PD/AG pretreatments (A) Venn diagram showing the intersections of genes hypermethylated in EBV-infected HCoEpC vs uninfected control cells (V vs. CT) and hypomethylated in EBV-infected HCoEpC pretreated with PAA or PD/AG versus EBV-infected cells (PAA-V vs.V and PD-AG-V vs.V, respectively). Genes were associated with DMRs using the Homer tool. The methylation mean of all DMRs associated with each gene was calculated and only genes that still had a methylation difference >20 % were considered. (B) Heatmaps showing the frequency of methylation of the 34 genes hypermethylated after EBV infection (V) and hypomethylated by pretreatment with PAA or with PD/AG (PAA-V and PD-AG-V, respectively). As a further control, PAA or PD/AG treatment of uninfected control cells is also shown. The color intensity is proportional to the methylation frequency: lighter colors indicate a low methylation level and vice versa. Grey cells indicate values that are not available. (C) Functional analysis of the common 34 genes on the Biological Processes database by using the GREAT R package. (D) Motif Enrichment Analysis (MEA) to identify proteins whose sequence binding motifs are enriched within the DMRs associated with the 34 genes mentioned above. For each DNA binding protein are reported the FDR-adjusted *p*-values, the frequency of related motif sequence found within the DMRs (target), the frequency within random sequences across the genome (background), and a logo plot with the consensus motif sequence.

functions were related to the regions whose methylation was altered by EBV, and by PAA or PD/AG pretreatment in infected cells, which were 1606, 1271 and 1015, respectively. To this aim, we performed a functional analysis using the Genomic Regions Enrichment of Annotations Tool (GREAT) R package. The heatmaps reported in Fig. 4 depict the significance levels as -log (FDR-adjusted *p*-value), with the darker color indicating the most significant enrichment results. We found that the regions whose methylation was altered by EBV in HCoEpC mainly affected genes regulating embryo development and morphogenesis, developmental process, negative regulation of apoptosis and RNA biosynthetic processes. These processes were enriched also in PAA-V versus V and, some of them, in PD/AG-V versus V, suggesting that PAA and partially PD/AG pretreatment could mitigate the effects induced by EBV on these processes. PAA treatment modulated some of these processes also in the control cells (Fig. 4A). After dissecting the regions hypermethylated (Fig. 4B) from those hypomethylated (Fig. 4C), we observed that RNA biosynthetic processes were enriched both in EBV-hypermethylated and hypomethylated regions and in those pretreated by PAA. The embryonic development processes were instead enriched only in the regions hypermethylated by the viral infection and in those pretreated with PAA, while the negative regulation of the apoptotic process was enriched in the regions hypermethylated by EBV and slightly in those pretreated with PAA (Fig. 4B). Finally, the cellular macromolecule biosynthetic processes were enriched in regions hypomethylated by EBV and in those pretreated by PAA (Fig. 4C). Overall, this analysis indicates that PAA was able to prevent EBV-induced perturbation of these processes more efficiently than PD/AG treatment, suggesting that other molecular pathway/s were also involved in the methylation changes induced by EBV in HCoEpC.

Focusing on molecular functions, we then found that the DMRs identified in all comparisons were involved in sequence-specific DNA binding (Fig. 4D) and that they were present both in hypermethylated

Table 1
Genomic regions differentially methylated with the relative methylation differences for each comparison of the 34 genes hypermethylated by EBV and hypomethylated by PAA, PD/AG or both pretreatments.

Gene Name	Annotation	TSS Distance	Position	V vs CT	PAA-V vs V	PD-AG-V vs V
MAEL	promoter-TSS	44	chr1:166975501–166,975,750	21.8	−21.4	−21.9
MAEL	promoter-TSS	294	chr1:166975751–166,976,000		−22.4	−23.6
ALX4	promoter-TSS	−737	chr11:44310751–44,311,000	34.1		−32.9
ALX4	Intergenic	−5987	chr11:44316001–44,316,250	27.0	−44.0	
ALX4	Intergenic	−6237	chr11:44316251–44,316,500	22.0	−33.2	
WNT11	Intergenic	−3124	chr11:76209501–76,209,750	23.1	−22.4	−21.7
WNT11	Intergenic	−3374	chr11:76209751–76,210,000			−30.8
MYO7A	intron	19,880	chr11:77148001–77,148,250			−27.3
MYO7A	exon	63,880	chr11:77192001–77,192,250	26.0	−27.8	
SCN8A	Intergenic	−54,107	chr12:51537001–51,537,250	35.0		
SCN8A	Intergenic	−22,857	chr12:51568251–51,568,500		−34.8	
SCN8A	Intergenic	−22,607	chr12:51568501–51,568,750		−32.4	
SCN8A	promoter-TSS	−357	chr12:51590751–51,591,000			−20.9
SCN8A	intron	140	chr12:51591251–51,591,500			−22.4
PLEKHG6	Intergenic	−32,060	chr12:6278251–6,278,500	24.1	−23.1	−24.4
PLEKHG6	Intergenic	−31,810	chr12:6278501–6,278,750	24.1	−21.3	−25.8
PLEKHG6	Intergenic	−31,560	chr12:6278751–6,279,000	24.1	−20.4	−24.5
FLT1	intron	1002	chr13:28494001–28,494,250	24.7		
FLT1	promoter-TSS	−498	chr13:28495501–28,495,750		−21.9	
FLT1	Intergenic	−37,248	chr13:28532251–28,532,500			−38.2
LINC02282	non-coding	−6589	chr14:28792251–28,792,500		−29.4	
LINC02282	Intergenic	−44,339	chr14:28830001–28,830,250	43.3		−46.8
LINC02282	Intergenic	−44,589	chr14:28830251–28,830,500			−40.9
IRF2BPL	exon	2582	chr14:77026001–77,026,250	25.6	−27.6	
IRF2BPL	exon	2332	chr14:77026251–77,026,500	27.5	−27.7	
IRF2BPL	exon	2082	chr14:77026501–77,026,750	24.4	−26.4	−37.9
HDGFL3	exon	447	chr15:83207251–83,207,500	28.9	−22.0	−32.8
HDGFL3	5' UTR	197	chr15:83207501–83,207,750	20.2		−25.0
ASIC2	promoter-TSS	−138	chr17:33293001–33,293,250		−20.2	
ASIC2	promoter-TSS	−388	chr17:33293251–33,293,500	22.9		−24.7
GJD3	exon	1611	chr17:40363001–40,363,250	22.1	−22.4	−23.8
GJD3	exon	1361	chr17:40363251–40,363,500		−20.5	−20.6
GJD3	exon	1111	chr17:40363501–40,363,750			−21.5
MRC2	promoter-TSS	−294	chr17:62627251–62,627,500	31.7	−34.0	−30.2
ASXL3	intron	657	chr18:33578751–33,579,000	36.4	−40.4	−36.4
ASXL3	intron	907	chr18:33579001–33,579,250	43.2		−41.8
ATP6V1C2	promoter-TSS	−254	chr2:10721251–10,721,500		−43.8	−47.4
ATP6V1C2	promoter-TSS	−4	chr2:10721501–10,721,750	40.5	−38.7	−37.9
ATP6V1C2	intron	246	chr2:10721751–10,722,000	36.8	−34.1	−31.1
INHBB	Intergenic	−1010	chr2:120345001–120,345,250		−22.9	−23.8
INHBB	promoter-TSS	−510	chr2:120345501–120,345,750		−21.3	−26.8
INHBB	promoter-TSS	−260	chr2:120345751–120,346,000	21.0	−29.4	
TMBIM1	intron	377	chr2:218292001–218,292,250	28.6		−31.6
TMBIM1	intron	127	chr2:218292251–218,292,500	40.7	−42.1	−39.3
TMBIM1	promoter-TSS	−49	chr2:218292501–218,292,750	36.0	−31.8	−36.8
DNER	intron	429	chr2:229714001–229,714,250	21.7		
DNER	exon	179	chr2:229714251–229,714,500		−22.6	
DNER	promoter-TSS	−71	chr2:229714501–229,714,750			−22.0
KCNK3	promoter-TSS	−96	chr2:26692501–26,692,750	35.6		−38.6
KCNK3	exon	154	chr2:26692751–26,693,000	40.0	−28.4	−39.3
KCNK3	exon	404	chr2:26693001–26,693,250	37.3	−26.6	−30.4
MIR663AHG	promoter-TSS	−143	chr20:26209251–26,209,500		−66.3	
MIR663AHG	promoter-TSS	−393	chr20:26209501–26,209,750		−65.7	
MIR663AHG	Intergenic	−641,893	chr20:26851001–26,851,250	33.5		−30.7
SLC32A1	promoter-TSS	−860	chr20:38723501–38,723,750			−28.7
SLC32A1	promoter-TSS	−610	chr20:38723751–38,724,000	20.6		
SLC32A1	intron	1640	chr20:38726001–38,726,250		−36.9	
LINC01990	intron	196	chr3:107431001–107,431,250		−26.8	
LINC01990	intron	446	chr3:107431251–107,431,500		−21.9	
LINC01990	intron	696	chr3:107431501–107,431,750	26.7	−26.8	−25.2
PEX5L	intron	31,849	chr3:179942251–179,942,500	26.7	−21.9	−38.0
PEX5L	intron	31,599	chr3:179942501–179,942,750		−32.0	−45.0
CHSY3	exon	411	chr5:129904751–129,905,000	30.3		−29.7
CHSY3	exon	661	chr5:129905001–129,905,250	38.0	−32.8	−31.9
CYSTM1	intron	188	chr5:140175251–140,175,500	23.2	−24.3	−23.6
GCNT4	promoter-TSS	−318	chr5:75052751–75,053,000	20.8	−24.1	−22.4
GCNT4	Intergenic	−1818	chr5:75054251–75,054,500			−24.8
FAM151B	promoter-TSS	−224	chr5:80487751–80,488,000	20.8	−20.3	−21.1
FAM151B	promoter-TSS	26	chr5:80488001–80,488,250	20.2		−21.2
MIR6720	TTS	285	chr6:1390001–1,390,250			−20.2
MIR6720	promoter-TSS	35	chr6:1390251–1,390,500	27.4	−25.1	
MIR6720	promoter-TSS	−215	chr6:1390501–1,390,750	29.9		
VGF	exon	−6557	chr7:101172001–101,172,250	34.5		−30.5

(*continued on next page*)

Table 1 (*continued*)

Gene Name	Annotation	TSS Distance	Position	V vs CT	PAA-V vs V	PD-AG-V vs V
VGF	exon	−6807	chr7:101172251–101,172,500	25.1	−20.8	−27.6
SP8	Intergenic	18,760	chr7:20768001–20,768,250	−20.1		
SP8	intron	260	chr7:20786501–20,786,750	39.9		
SP8	promoter-TSS	10	chr7:20786751–20,787,000	32.4		
SP8	promoter-TSS	−240	chr7:20787001–20,787,250	38.3		
SP8	Intergenic	−11,240	chr7:20798001–20,798,250	21.1	−26.8	−21.6
SP8	Intergenic	−11,490	chr7:20798251–20,798,500	31.4	−35.1	−32.5
SP8	Intergenic	−11,740	chr7:20798501–20,798,750	42.3	−43.1	−44.6
HSPB1	intron	−20,047	chr7:76282501–76,282,750	23.8	−23.4	−23.1
HSPB1	intron	−19,797	chr7:76282751–76,283,000	29.8		−29.3
HSPB1	intron	−19,547	chr7:76283001–76,283,250	27.3		
PPP1R9A	intron	489	chr7:94908001–94,908,250	54.3	−38.9	−50.0
KCNV1	exon	1645	chr8:109974001–109,974,250	32.0	−39.9	−28.7
KCNV1	exon	1395	chr8:109974251–109,974,500	32.0	−40.1	−29.2
CA8	intron	524	chr8:60280751–60,281,000	21.3		−31.1
CA8	promoter-TSS	24	chr8:60281251–60,281,500	24.4	−22.5	−24.2
CA8	promoter-TSS	−226	chr8:60281501–60,281,750		−24.0	−26.1

(Fig. 4E) and hypomethylated regions (Fig. 4F).

3.4. Insights into genes hypermethylated by EBV and hypomethylated by PAA or PD/AG pretreatments

Since EBV primarily drove hypermethylation, we further assessed how many and which genes were hypermethylated by viral infection and hypomethylated by PAA or PD/AG pretreatments in HCoEpC. As shown in Fig. 5A, we found that 703 genes were hypermethylated by EBV infection, 137 of which were hypomethylated by PAA, 100 by PD/AG, and 34 by both PAA and PD/AG pretreatments. The methylation levels of the 34 genes hypermethylated by EBV and hypomethylated by PAA or PD/AG pretreatments are represented in the heatmap shown in Fig. 5B, while the genomic regions and the relative methylation difference for each comparison of these genes are reported in Table 1. To investigate the biological role of these 34 genes, a functional analysis was performed by using the GREAT R package in the Biological Processes database. Interestingly, we observed that among the genes hypermethylated by EBV infection and hypomethylated by both pretreatments there were those involved in embryogenesis, VEGF signaling pathway and negative regulation of the Fas pathway (Fig. 5C), which could play a role in promoting EBV-driven inflammation and carcinogenesis [24,25]. Then, to identify DNA binding proteins that could bind to enriched DNA sites within the DMRs associated with these 34 genes, we performed Motif Enrichment Analysis (MEA) (Fig. 5D). Indeed, variation in the level of methylation within these regions may positively or negatively influence the recruitment of DNA-binding proteins. We found that 13 sequence motifs were statistically enriched (adjustedp-value < 0.05) within the DMRs. Of note, among these, we found the binding sequence motif of STAT2, which has been shown to be degraded by an EBV lytic protein to prevent the interferon signaling [26], suggesting that the virus could influence STAT2 activity also through epigenetic changes. Furthermore, methylation was changed in the binding region of early B cell factor 1 (EBF1), previously shown to be epigenetically silenced in gastric carcinoma [27], and of Yin Yang 2 (YY2), that may counterbalance the oncogenic effects of YY1 [28] (Fig. 5D).

Insights into genes hypomethylated by EBV and hypermethylated by PAA or PD/AG pretreatments.

We finally evaluated which genes were hypomethylated by EBV and hypermethylated by PAA, PD/AG or both pretreatments. We found that 476 genes were hypomethylated by EBV, of which 107 were hypermethylated by PAA, 71 by PD/AG and 26 by both pretreatments (Fig. 6A). The methylation levels of these 26 genes are depicted in the heat maps shown in Fig. 6B, while the genomic regions and relative methylation difference for each comparison of these 26 genes are reported in Table 2. To investigate the biological role of these genes, a functional analysis was performed by using the GREAT R package on the Biological Processes database. We observed that genes hypermethylated by EBV infection and hypomethylated by both treatments included those involved in the negative regulation of epithelial cell migration and in the regulation of epithelial regeneration (Fig. 6C). Next, by performing Motif Enrichment Analysis (MEA), we identified several proteins that could bind to enriched DNA binding sites within the DMRs associated with these 26 genes. Among those, SMAD3 and MEF2A, proteins involved in epithelial–mesenchymal transition (EMT) and tumor progression [29,30] (Fig. 6D), whose altered methylation could contribute to EBV-driven carcinogenesis.

HOX and WNT are among the genes whose methylation is modified by EBV infection.

Based on the observation that EBV was mainly driving hypermethylation in HCoEpC and on previous findings showing that this effect could contribute to viral-driven tumorigenesis [17], we first focused on the genes hypermethylated by the virus in HCoEpC. We found that hypermethylation mainly affected genes encoding transcription factors such as homeobox (HOX) genes (Table 3).

Interestingly, in the case of HOXB2, HOXA3, and HOXB4, we noticed that the regions hypermethylated by EBV were the same that were hypomethylated by PAA pretreatment (Table 3). Regarding HOXB4, we observed that EBV hypermethylated it in the exon located in the position chr17:48576751:48577000 and in the intron located in chr17:48577001:48577250 and that PAA pretreatment hypomethylated the exon in the same position while the intron was not affected (Fig. 7A and B and Table 3). Conversely, PD/AG did not change the methylation landscape induced by EBV on HOXB4, both in the exon and intron, as reported in Table 3 and shown in Fig. 7A. Furthermore, by RT-qPCR performed on HOXB4 we found that its expression was upregulated by EBV infection and that such upregulation was prevented by PAA while it was not affected by PD/AG (Fig. 7B), according to the effect observed on methylation. Interestingly, the expression of HOX is closely related to that of WNT genes, since WNT proteins have been reported to trigger HOX activation [31]. Accordingly, here we observed that several WNT genes were also hypermethylated by EBV (Table 3) and that one of them, namely WNT11, was hypermethylated by EBV in the intergenic region located in the chr11:76209501–76,209,750 position, and hypomethylated in the same position by both PAA or PD/AG pretreatments (Table 3 and Fig. 8A). In agreement, RT-qPCR performed on WNT11, showed that its expression was upregulated by EBV infection and counteracted by both PAA or PD/AG pretreatments (Fig. 8B), suggesting a concomitant effects of these drugs both on methylation and expression of this gene. The upregulated expression of HOXB4 and WNT11 in EBV-infected cells was counteracted by 5-AZA pretreatment (Supplementary Fig.S4A and B), further suggesting that these effects occurred in correlation with the hypermethylation of these genes. These results are also in agreement

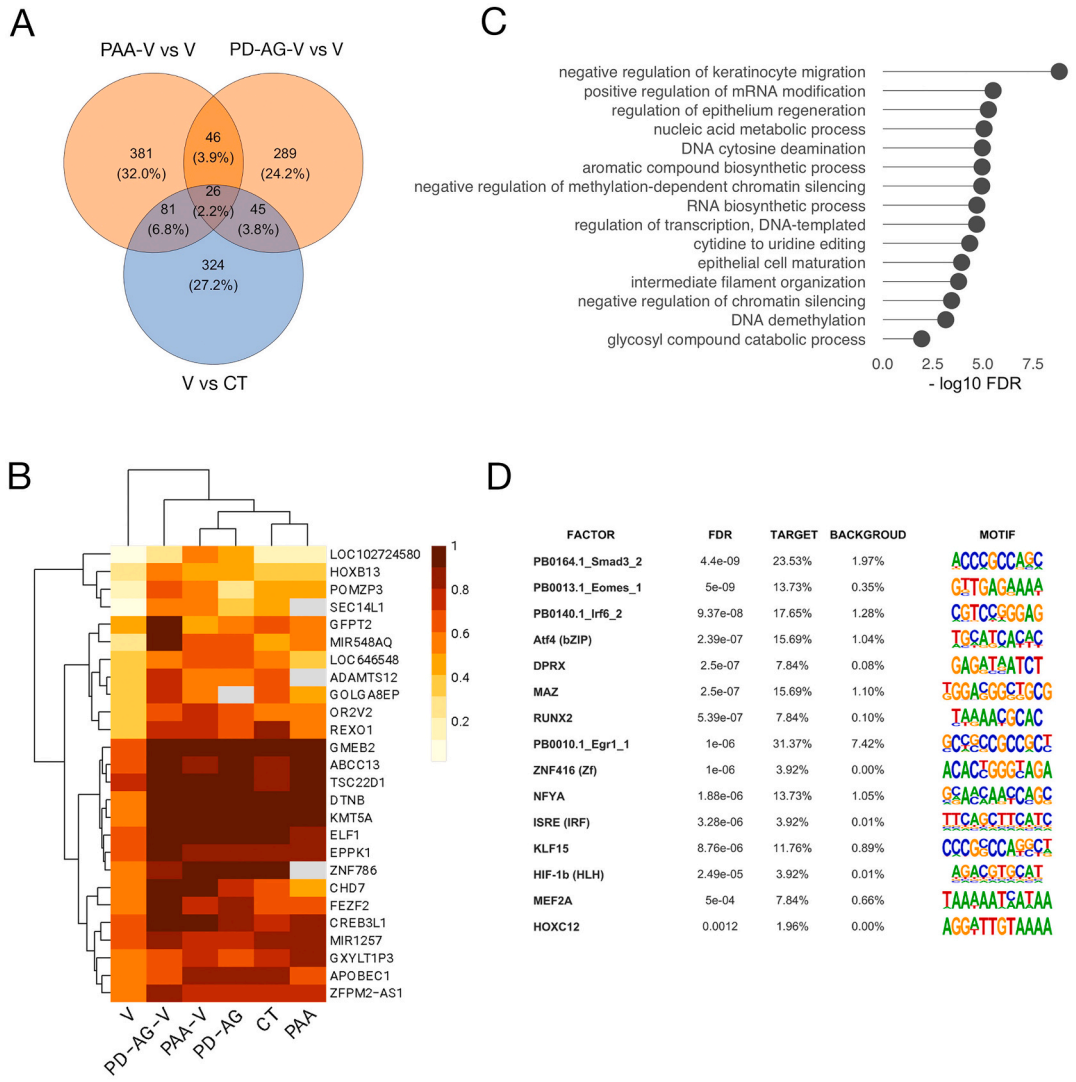

Fig. 6. Genes hypomethylated by EBV and hypermethylated by PAA or PD/AG pretreatments (A) Venn diagram depicting the intersections of genes hypomethylated in EBV-infected HCoEpC vs uninfected control cells (V vs. CT) and hypermethylated in EBV-infected HCoEpC pretreated with PAA or PD/AG versus EBV-infected cells (PAA-V vs.V and PD-AG-V vs.V, respectively). Genes were associated with DMRs using the Homer tool. The methylation mean of all DMRs associated with each gene was calculated and only genes that still had a methylation difference >20 % were considered. (B) Heatmaps showing the frequency of methylation of the 26 genes hypomethylated after EBV infection (V) and hypermethylated by pretreatment with PAA or with PD/AG (PAA-V and PD-AG-V, respectively). As a further control, PAA or PD/AG treatment of uninfected control cells is also shown. The color intensity is proportional to the methylation frequency: lighter colors indicate a low methylation level and vice versa. Grey cells indicate values that are not available. (C) Functional analysis of the 26 common DMRs on the Biological Processes database by using the GREAT R package. (D) Motif Enrichment Analysis (MEA) to identify proteins whose sequence binding motifs are enriched within the DMRs associated with the 26 genes mentioned above. For each DNA binding protein are reported the FDR-adjusted p-values, the frequency of related motif sequence found within the DMRs (target), the frequency within random sequences across the genome (background), and a logo plot with the consensus motif sequence.

with the current literature suggesting that methylation of regions other than promoters may be associated with an increased gene expression rather than silencing [32–34].

4. Discussion

A better understanding of the impact that EBV infection may have on DNA methylation of host cell genome, the genes affected by this epigenetic modification and the molecular mechanisms that regulate it, could help achieve better control over the onset of EBV-driven malignancies. Indeed, epigenetic modifications play a key role in oncogenesis, together with genetic mutations but, unlike the latter, they can be reversed with appropriate therapeutic approaches [11,35]. However, to what extent dysregulated methylation may contribute to cancer depends on the tumor type, and gastric and colon cancers are among those in which methylation changes play an important role [36,37]. Furthermore, aberrant methylation is involved in the pathogenesis of IBD, as demonstrated by an integrative epigenome-wide analysis (37), and interestingly, some forms of these inflammatory diseases have been associated with EBV [2,3]. This virus is strongly linked to several cancers, either of hematological and epithelial origin, including gastric cancer, and aberrant methylation contributes to viral-driven tumorigenesis [10]. For example, in gastric cancer cells, it has been reported that the EBV protein LMP2A activates STAT3 and ERK1/2, upregulating DNMTs, and that these effects result in the silencing of tumor suppressor genes such as PTEN [38]. However, in EBV-associated tumor cells, the viral infection may have occurred for a long time and the virus is present mainly in a latent state, which is different from primary infection of non-tumor epithelial cells, in which the virus usually replicates before the latency is established (39). In fact, tumor cell lines do not allow us to evaluate which genes are aberrantly methylated and could play a role in the early stages of oncogenic transformation, since tumor cells represent

Table 2
Genomic regions and relative methylation difference for each comparison of the 26 genes hypomethylated by EBV and hypermethylated by PAA, PD/AG or both pretreatments.

Gene name	Annotation	TSS Distance	Position	V vs CT	PAA-V vs V	PD-AG-V vs V
CREB3L1	intron	2464	chr11:46280001–46,280,250		33.3	29.3
CREB3L1	intron	24,464	chr11:46302001–46,302,250	−30.0	30.2	32.6
MIR548AQ	Intergenic	−6403	chr12:121590001–121,590,250	−20.3	38.1	
KMT5A	Intergenic	−8506	chr12:123375501–123,375,750	−33.0	34.8	31.3
APOBEC1	Intergenic	42,282	chr12:7623501–7,623,750			20.8
APOBEC1	Intergenic	37,282	chr12:7628501–7,628,750	−36.8	45.5	24.1
APOBEC1	Intergenic	37,032	chr12:7628751–7,629,000	−30.2	26.8	
APOBEC1	Intergenic	−12,277	chr12:7682751–7,683,000	−21.9		
ELF1	intron	26,406	chr13:40955751–40,956,000	−28.0	30.1	29.6
ELF1	intron	26,156	chr13:40956001–40,956,250	−34.0	31.3	
TSC22D1	Intergenic	−14,061	chr13:44590501–44,590,750	−31.2	24.0	32.9
LOC646548	intron	768	chr14:70187751–70,188,000	−26.8	34.4	30.3
GOLGA8EP	Intergenic	19,400	chr15:22418501–22,418,750	−36.8		48.3
GOLGA8EP	Intergenic	19,150	chr15:22418751–22,419,000	−25.1	32.4	45.5
HOXB13	5' UTR	123	chr17:48728501–48,728,750			32.4
HOXB13	Intergenic	−4377	chr17:48733001–48,733,250		31.9	
HOXB13	Intergenic	−4627	chr17:48733251–48,733,500		23.8	
HOXB13	Intergenic	−10,377	chr17:48739001–48,739,250	−36.0	22.6	
SEC14L1	intron	6157	chr17:77147001–77,147,250	−42.1	50.4	67.0
REXO1	TTS	−3643	chr19:1852001–1,852,250	−50.7	39.2	39.2
REXO1	exon	−6143	chr19:1854501–1,854,750		39.4	
DTNB	intron	77,096	chr2:25573001–25,573,250	−37.3	34.2	38.8
MIR1257	Intergenic	11,536	chr20:61942001–61,942,250		36.4	
MIR1257	Intergenic	−17,714	chr20:61971251–61,971,500	−29.9		30.8
MIR1257	Intergenic	−17,964	chr20:61971501–61,971,750	−28.2		
GMEB2	intron	4225	chr20:63622751–63,623,000	−28.2	26.2	26.8
ABCC13	Intergenic	47,827	chr21:14321501–14,321,750	−26.4	30.3	
ABCC13	Intergenic	48,077	chr21:14321751–14,322,000			22.7
MIR548AQ	intron	27,028	chr3:185740751–185,741,000		23.9	26.4
FEZF2	exon	1174	chr3:62372251–62,372,500		35.3	
FEZF2	intron	−220,826	chr3:62594251–62,594,500	−22.8		21.4
GFPT2	intron	30,210	chr5:180323001–180,323,250	−23.9	27.2	22.4
GFPT2	intron	29,960	chr5:180323251–180,323,500	−21.9		
OR2V2	Intergenic	7433	chr5:181162251–181,162,500	−22.4		
OR2V2	Intergenic	14,933	chr5:181169751–181,170,000		43.1	
OR2V2	Intergenic	15,183	chr5:181170001–181,170,250		42.8	44.4
OR2V2	Intergenic	15,433	chr5:181170251–181,170,500		39.2	
ADAMTS12	promoter-TSS	−136	chr5:33892001–33,892,250	−26.6	31.9	35.6
ZNF786	TTS	−11,158	chr7:149101751–149,102,000	−32.2	34.0	29.5
POMZP3	intron	27,677	chr7:76599501–76,599,750	−29.7	35.8	48.3
ZFPM2-AS1	Intergenic	−4873	chr8:106065251–106,065,500	−61.1	58.9	45.6
EPPK1	exon	14,588	chr8:143863751–143,864,000	−20.3	23.2	
EPPK1	exon	12,088	chr8:143866251–143,866,500	−31.0	30.6	32.9
EPPK1	exon	9588	chr8:143868751–143,869,000			33.3
EPPK1	intron	3838	chr8:143874501–143,874,750		27.0	
CHD7	Intergenic	−36,364	chr8:60642251–60,642,500	−28.0	25.7	23.0
CHD7	exon	617	chr8:60741751–60,742,000		20.9	
GXYLT1P3	non-coding	127	chr9:40348501–40,348,750	−22.8	29.9	
GXYLT1P3	non-coding	377	chr9:40348751–40,349,000	−36.5	55.1	39.3
LOC102724580	Intergenic	83,645	chr9:40583501–40,583,750	−36.0	70.0	40.6
LOC102724580	Intergenic	84,145	chr9:40584001–40,584,250	−29.6		

the final products of a transformation process. A previous study has overcome this problem and investigated the impact of EBV infection on genome-wide DNA methylation in a model of immortalized normal gastric epithelial cell line [39], which however may be still quite different from primary epithelial cells.

EBV has been associated with IBD, particularly with the forms more resistant to therapies [2] and a possible link between the virus and colon carcinogenesis has also been suggested [8]. At this regard, we have recently reported that EBV infection of primary colonic cells (HCoEpC) promoted inflammation and induced an impairment of autophagy and DDR, pro-tumorigenic effects to which contributed an altered DNA methylation [17]. EBV-infected HCoEpC may represent a suitable model to investigate the methylation changes induced by viral infection of primary epithelial cells as possible mechanism contributing to driving inflammation and carcinogenesis. Therefore, in this study, we performed a genome-wide methylome analysis on EBV-infected and uninfected HCoEpC, utilizing the Oxford Nanopore Technologies (ONT). This platform enables a direct measurement of the base epigenetic mark alongside nucleotide sequencing, avoiding chemical treatments such as bisulfite conversion and PCR potential artifacts. Nanopore technology also enables the sequencing of long reads [40,41] and highly repetitive regions of the human genome, difficult or in some cases impossible to perform with the short reads widely used sequencing methods [40,42].

The results obtained here suggest that EBV infection induced methylation changes in HCoEpC and that it drove DNA hypermethylation over hypomethylation. Intriguingly, a global increase of DNA methylation has been observed at the earliest stages of colon tumor initiation [43], and EBV infection may be, in some cases, involved in this epigenetic change. Also because previous studies have shown that aberrant DNA methylation of tumor-related genes plays a role in the development and progression of EBV-associated gastric cancer [44] and that the methyl groups added by EBV to the non-neoplastic cell line genome represent a long-lasting epigenetic modification [39]. Moreover, chronic intestinal inflammatory diseases such as IBD, in some cases associated with EBV [2], are characterized by aberrant methylation, so that this epigenetic modification has been proposed as a potential

Table 3
Impact of EBV infection and PAA treatment on the methylation levels of the HOX and WNT genes. All the DMRs of these gene-families are listed.

Gene Name	Annotation	TSS Distance	Position	V vs CT	PAA-V vs V	PD-AG-V vs V
HOXA3	intron	5969	chr7:27113501–27,113,750	26.3	−30.2	
HOXA3	intron	5719	chr7:27113751–27,114,000	20.5		
HOXA3	intron	5469	chr7:27114001–27,114,250	25.4		
HOXA6	intron	−3102	chr7:27150751–27,151,000	−21.7		
HOXA6	intron	−3352	chr7:27151001–27,151,250	−22.3		
HOXB2	intron	−10,595	chr17:48555501–48,555,750	24.8	−23.8	
HOXB3	intron	10,072	chr17:48564251–48,564,500		20.1	
HOXB3	intron	9822	chr17:48564501–48,564,750	−33.4	22.9	
HOXB3	3' UTR	−1529	chr17:48576501–48,576,750	33.4		
HOXB3	Intergenic	−2497	chr17:48584751–48,585,000		38.0	
HOXB4	exon	1474	chr17:48576751–48,577,000	46.6	−56.8	
HOXB4	intron	1224	chr17:48577001–48,577,250	48.2		
HOXC12	Intergenic	5973	chr12:53960751–53,961,000	−23.8		
HOXC12	Intergenic	6223	chr12:53961001–53,961,250		24.3	
HOXC12	TTS	6473	chr12:53961251–53,961,500	−32.0	21.9	
HOXD13	exon	405	chr2:176093001–176,093,250	20.1		
PHOX2B	Intergenic	−2906	chr4:41751751–41,752,000	25.9		
WNT1	promoter-TSS	−196	chr12:48978001–48,978,250		−20.5	
WNT1	intron	1554	chr12:48979751–48,980,000	21.1		
WNT1	intron	1804	chr12:48980001–48,980,250	36.9		
WNT1	intron	2054	chr12:48980251–48,980,500	32.1		
WNT1	intron	2804	chr12:48981001–48,981,250	24.2	−40.0	
WNT1	exon	3054	chr12:48981251–48,981,500		−29.4	
WNT10A	intron	−8976	chr2:218871751–218,872,000		−45.7	
WNT10A	intron	2774	chr2:218883501–218,883,750	47.6		
WNT11	Intergenic	−3124	chr11:76209501–76,209,750	23.1	−22.4	−21.7
WNT11	Intergenic	−3374	chr11:76209751–76,210,000			−30.8
WNT2B	5' UTR	161	chr1:112509001–112,509,250	26.3		
WNT2B	exon	411	chr1:112509251–112,509,500	20.8		
WNT5B	intron	−5855	chr12:1623251–1,623,500	−20.2		
WNT8A	Intergenic	−15,266	chr5:138068501–138,068,750	28.4		
WNT9A	intron	1056	chr1:227946751–227,947,000	35.8		

biomarker to identify these pathological conditions [14].

In a previous study, we have shown that the inhibition of late lytic EBV antigen expression by PAA counteracted most of the pro-tumorigenic effects induced by EBV in HCoEpC [17], supporting the previously suggested role of lytic antigens in triggering EBV-induced carcinogenesis [45,46]. In line with these results, here we found that PAA prevented several methylation changes induced by the virus. In line with our results, it has been reported that also other viruses linked to human cancer, e.g. hepatitis B virus, upregulated DNMTs to induce abnormal transcription activation and genomic instability during the replicative cycle [47]. The activation of ERK1/2 and STAT3, that were found to contribute to dysregulate methylation in viral-infected HCoEpC, have been reported to be strongly involved in methylation changes in EBV-associated tumor cells [9]. For example LMP2A, which we found to be expressed in EBV-infected HCoEpC, was detected in approximately 40 % of gastric cancer patients [48] and shown to upregulate DNMT1 [49], in correlation with the phosphorylation of STAT3 [50]. LMP2A has also been reported to induce ERK1/2 phosphorylation, leading to the upregulation of DNMTs [10].

From the analysis of the biological processes related to the genes whose methylation was altered by EBV, it emerges that viral infection affected several genes such as HOX.

HOX genes have been reported to be differentially regulated at the level of DNA methylation in proximal and distal colon segments. This difference may be implicated in inflammatory bowel disease such as ulcerative colitis occurring in distal colon segment in which HOX B genes are hypermethylated [51].

Both HOX and WNT strongly involved in the regulation of embryogenesis and developmental processes.

Notably, embryogenesis and oncogenesis share many similarities, as indeed adult cells de-re-programmed to a ground state become similar to cancer stem cells and become thus capable of generating tumors [52]. The aberrant methylation of genes regulating these processes could thus play a role in epithelial cancer onset, as they may contribute to reprogram cells, allowing to initiate the oncogenic transformation. In accordance to our data, the altered methylation of multiple genes characterizes the CpG Island Methylator Phenotype typical of EBV-positive gastric carcinoma [53].

Some HOX genes have been also reported to promote chronic inflammation, given that NF-kB and HOX proteins can regulate each other through several mechanisms, including reciprocal transcriptional regulation, protein-protein interactions, and control of upstream and downstream interactors [54]. Wnt signaling is also involved in chronic inflammatory diseases' pathogenesis including cancer-related inflammation, as it is involved in the control of inflammatory cytokine production [55]. Regarding colon, it has been reported that aberrant Wnt signaling is observed in multiple intestinal inflammatory diseases, including inflammatory bowel disease (IBD) and IBD-associated colon cancer [56]. Besides HOX and WNT, EBV hypermethylated other genes regulating embryogenesis such as Forkhead box (Fox), sine oculis (SIX), sex-determining region Y (Sry) box-containing factor (Sox) and PAX (data not shown) [57–61]. These genes regulate key cellular processes such as cell proliferation, death and differentiation, as well as angiogenesis, autophagy and cell receptor signaling [57]. Interestingly, an altered methylation of genes affecting tissue-specific differentiation has been reported to be the predominant mechanism by which epigenetic changes lead to the onset colon cancer [62], highlighting the important pathogenetic role that their aberrant methylation may have in these cells.

Also because, when focusing on HOXB4 and WNT11, two genes hypermethylated by EBV in an exon or in the intergenic region, respectively, we found that they were upregulated in infected HCoEpC and that PAA or PD/AG prevented the hypermethylation and counteracted such upregulation, suggesting a link between these effects. Hypermethylation in the promoter regions generally reduces gene expression, playing a key role for example in the silencing of tumor suppressor genes, while methylation changes occurring in other genomic regions may differently regulate gene expression [63], also for

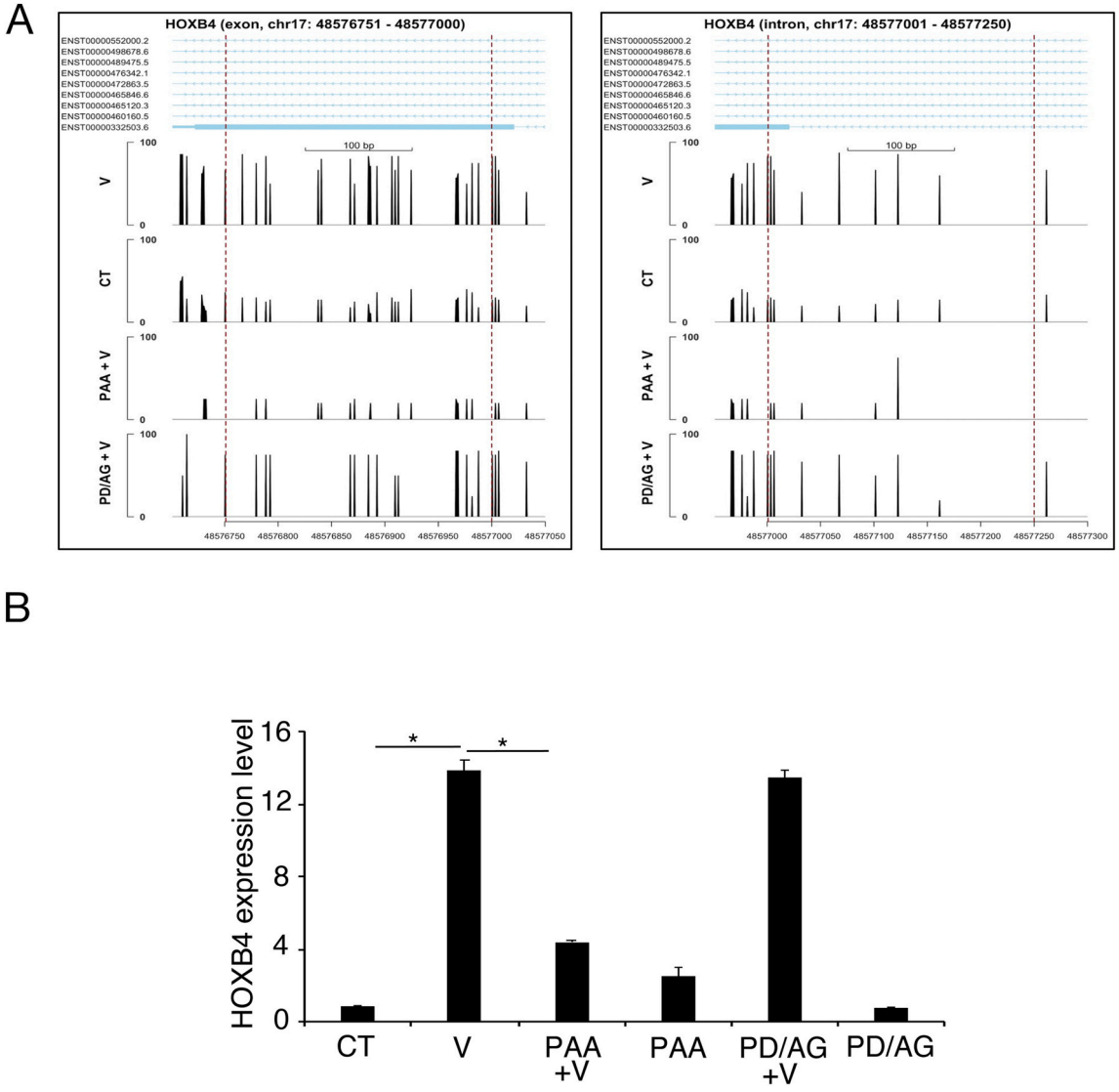

Fig. 7. EBV infection of HCoEpC induces methylation changes in an exon of HOXB4 resulting in positive regulation of its expression, and PAA treatment prevents both effects. (A) Genomic visualization of two HOXB4 DMRs with the methylation levels on the y-axis for each condition. Above are reported the transcripts of HOXB4 with introns as arrows and exons as solid rectangles (B) RT-qPCR was performed to analyze the expression level of HOXB4 in uninfected control (CT) and EBV-infected (V) HCoEpC pretreated with PAA (PAA + V) or with PD/AG (PD/AG + V) as well as in uninfected control treated or not with PAA (PAA) or with PD/AG (PD/AG). One representative experiment is shown and histograms represent the mean plus SD of three different experiments.

example by prevent the binding of transcriptional repressors such as in the case of CTCF [64] or activators [65]. However, the outcome of DNA methylation on gene expression is still being studied and this topic is further complicated by the interaction that DNA methylation can have with other epigenetic modifications such as histone methylation and acetylation [66–68].

The Motif Enrichment Analysis (MEA), that we also performed in this study, led to the identification of several proteins that could bind to enriched DNA sites within the DMRs. Among those, again molecules involved in cancer such EBF1, which is a TERT transcriptional repressor and whose inactivation represents the major cause of TERT upregulation, TCF7 which regulates migration and invasion of CRC cells, and SMAD3 that is strongly involved in epithelial–mesenchymal transition (EMT) [27,29,69].

In conclusion, this study helps to shed light on the impact that EBV infection can have on DNA methylation in primary colon epithelial cells and identifies some processes and genes affected by this epigenetic modification. It emerges that methylation affected several genes involved in inflammation, embryogenesis and carcinogenesis, suggesting that EBV was able to reprogram these cells. Furthermore, as EBV induced methylation changes in genes encoding Long non-coding RNA (lncRNA) and MicroRNAs (miRNAs) (Tables 1 and 2), this effect may induce other epigenetic changes [70,71]. Overall, the results of this study suggest that strategies capable of interfering with DNA methylation could help counteract the onset of EBV-associated pathologies affecting colon epithelia. This could also suggest that, as for another DNA virus closely linked to human cancer, namely the Human Papillomavirus (HPV), for which DNA methylation can be considered a biomarker of disease progression (64), methylation changes could help identify EBV-associated forms of IBD that possibly progress to colon cancer.

Supplementary data to this article can be found online at https://doi.org/10.1016/j.bbagrm.2024.195064.

Data are available using the GEO Code GSE272423

Funding information

This work was supported by the Italian Association for Cancer

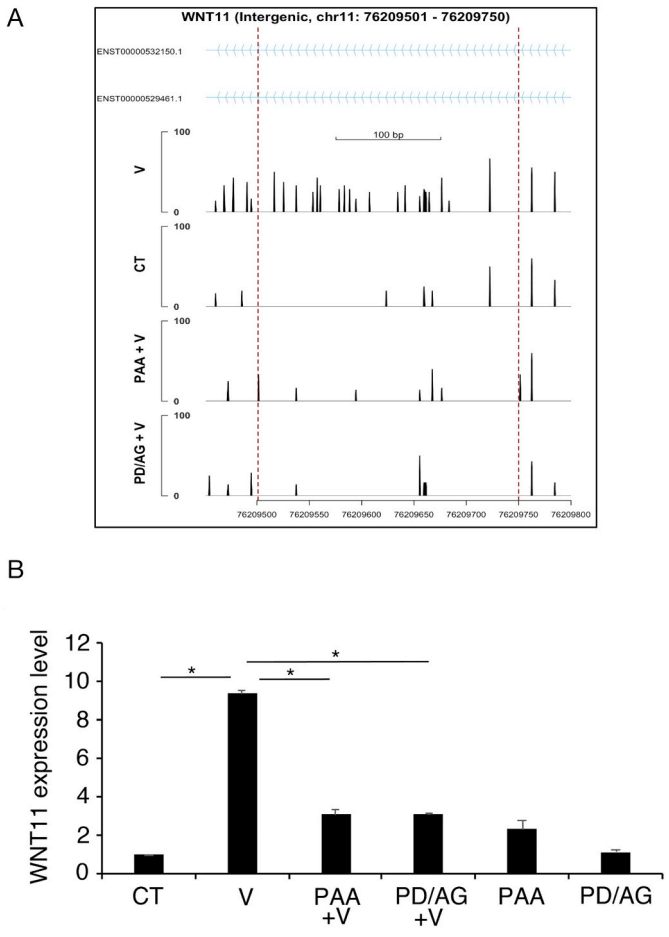

Fig. 8. EBV infection of HCoEpC induces methylation changes in the intergenic region of WNT11 resulting in positive regulation of its expression level, and both effects are prevented by PAA or PD/AG pretreatments. (A) Genomic visualization of the intergenic DMR of WINT11 with the methylation levels on the y-axis for each condition. Above are reported the transcripts of HOXB4 with introns depicted as arrows (B) RT-qPCR was performed to assess the expression level of WNT11 in uninfected control (CT) and EBV-infected (V) HCoEpC pretreated with PAA (PAA + V) or with PD/AG (PD/AG + V) as well as in uninfected control treated or not with PAA (PAA) or with PD/AG (PD/AG). One representative experiment is shown and histograms represent the mean plus SD of three different experiments.

Research (AIRC; grant IG 2019 Id.23040), PRIN2017 (2017K55HLC) and by ATENEO 2020-21.

Author statement

We declare that this manuscript is original, has not been published before and is not currently being considered for publication elsewhere.

CRediT authorship contribution statement

Giuseppe Rubens Pascucci: Validation, Software, Methodology, Formal analysis, Data curation. **Salvatore Lo Presti:** Investigation. **Michele Di Crosta:** Investigation. **Rossella Benedetti:** Investigation. **Alessia Neri:** Investigation. **Roberta Gonnella:** Writing – review & editing, Writing – original draft, Validation, Methodology, Investigation, Formal analysis, Data curation, Conceptualization. **Mara Cirone:** Writing – review & editing, Writing – original draft, Supervision, Resources, Funding acquisition, Data curation, Conceptualization.

Declaration of competing interest

The authors declare that they have no known competing financial interests or personal relationships that could have appeared to influence the work reported in this paper.

Data availability

Data will be made available on request.

Acknowledgement

The authors thank Dr. Marta Rebuzzi for technical assistance.

References

[1] P.J. Farrell, Epstein-Barr virus and Cancer, Annu. Rev. Pathol. 14 (2019) 29–53.
[2] R. Ciccocioppo, F. Racca, L. Scudeller, A. Piralla, P. Formagnana, L. Pozzi, E. Betti, A. Vanoli, R. Riboni, P. Kruzliak, F. Baldanti, G.R. Corazza, Differential cellular localization of Epstein-Barr virus and human cytomegalovirus in the colonic mucosa of patients with active or quiescent inflammatory bowel disease, Immunol. Res. 64 (2016) 191–203.
[3] H. Zhang, S. Zhao, Z. Cao, Impact of Epstein-Barr virus infection in patients with inflammatory bowel disease, Front. Immunol. 13 (2022) 1001055.
[4] J.E. Axelrad, S. Lichtiger, V. Yajnik, Inflammatory bowel disease and cancer: the role of inflammation, immunosuppression, and cancer treatment, World J. Gastroenterol. 22 (2016) 4794–4801.
[5] K. Matsusaka, S. Funata, M. Fukayama, A. Kaneda, DNA methylation in gastric cancer, related to helicobacter pylori and Epstein-Barr virus, World J. Gastroenterol. 20 (2014) 3916–3926.
[6] E. Jafari Maskouni, T. Jamalvandi, F. Tabatabaei, S. Bourenjan Shirazi, H. Saadati, A. Letafati, M. Hosseini, S. Motlaghzadeh, Z. Khalesi, P. Moradi, S. Saeb, N. Sheikh, E. Fozouni, A. Khatami, A.H. Baker, Z. Keyvanlou, V. Tamrchi, A. Tavakoli, S. Ghorbani, Association between Epstein-Bar virus and colorectal cancer: a systematic review and meta-analysis, Microb. Pathog. 179 (2023) 106087.
[7] W. Xu, X. Jiang, J. Chen, Q. Mao, X. Zhao, X. Sun, L. Zhong, L. Rong, Chronic active Epstein-Barr virus infection involving gastrointestinal tract mimicking inflammatory bowel disease, BMC Gastroenterol. 20 (2020) 257.
[8] S. Bedri, A.A. Sultan, M. Alkhalaf, A.E. Al Moustafa, S. Vranic, Epstein-Barr virus (EBV) status in colorectal cancer: a mini review, Hum. Vaccin. Immunother. 15 (2019) 603–610.
[9] M.M.L. Leong, M.L. Lung, The impact of Epstein-Barr virus infection on epigenetic regulation of host cell gene expression in epithelial and lymphocytic malignancies, Front. Oncol. 11 (2021) 629780.
[10] L. Zhang, R. Wang, Z. Xie, The roles of DNA methylation on the promotor of the Epstein-Barr virus (EBV) gene and the genome in patients with EBV-associated diseases, Appl. Microbiol. Biotechnol. 106 (2022) 4413–4426.
[11] L.D. Moore, T. Le, G. Fan, DNA methylation and its basic function, Neuropsychopharmacology 38 (2013) 23–38.
[12] H. Meng, Y. Cao, J. Qin, X. Song, Q. Zhang, Y. Shi, L. Cao, DNA methylation, its mediators and genome integrity, Int. J. Biol. Sci. 11 (2015) 604–617.
[13] J. Xu, H.M. Xu, M.F. Yang, Y.J. Liang, Q.Z. Peng, Y. Zhang, C.M. Tian, L.S. Wang, J. Yao, Y.Q. Nie, D.F. Li, New insights into the epigenetic regulation of inflammatory bowel disease, Front. Pharmacol. 13 (2022) 813659.
[14] I. Agliata, N. Fernandez-Jimenez, C. Goldsmith, J.C. Marie, J.R. Bilbao, R. Dante, H. Hernandez-Vargas, The DNA methylome of inflammatory bowel disease (IBD) reflects intrinsic and extrinsic factors in intestinal mucosal cells, Epigenetics 15 (2020) 1068–1082.
[15] R. Lakshminarasimhan, G. Liang, The role of DNA methylation in Cancer, Adv. Exp. Med. Biol. 945 (2016) 151–172.
[16] V. Pietropaolo, C. Prezioso, U. Moens, Role of virus-induced host cell epigenetic changes in Cancer, Int. J. Mol. Sci. 22 (2021).
[17] R. Santarelli, L. Evangelista, C. Pompili, S. Lo Presti, A. Rossi, A. Arena, A. Gaeta, R. Gonnella, M.S. Gilardini Montani, M. Cirone, EBV infection of primary colonic epithelial cells causes inflammation, DDR and autophagy dysregulation, effects that may predispose to IBD and carcinogenesis, Virus Res. 338 (2023) 199236.
[18] S. Heinz, C. Benner, N. Spann, E. Bertolino, Y.C. Lin, P. Laslo, J.X. Cheng, C. Murre, H. Singh, C.K. Glass, Simple combinations of lineage-determining transcription factors prime cis-regulatory elements required for macrophage and B cell identities, Mol. Cell 38 (2010) 576–589.
[19] R.C. Team, R: A Language and Environment for Statistical Computing, 2022.
[20] Z. Gu, D. Hubschmann, rGREAT: an R/bioconductor package for functional enrichment on genomic regions, Bioinformatics 39 (2023).
[21] M. Rowe, B. Glaunsinger, D. van Leeuwen, J. Zuo, D. Sweetman, D. Ganem, J. Middeldorp, E.J. Wiertz, M.E. Ressing, Host shutoff during productive Epstein-Barr virus infection is mediated by BGLF5 and may contribute to immune evasion, Proc. Natl. Acad. Sci. U. S. A. 104 (2007) 3366–3371.
[22] M.T. McIntosh, S. Koganti, J.L. Boatwright, X. Li, S.V. Spadaro, A.C. Brantly, J. B. Ayers, R.D. Perez, E.M. Burton, S. Burgula, T. MacCarthy, S. Bhaduri-McIntosh, STAT3 imparts BRCAness by impairing homologous recombination repair in Epstein-Barr virus-transformed B lymphocytes, PLoS Pathog. 16 (2020) e1008849.

[23] M. Granato, M.S. Gilardini Montani, C. Zompetta, R. Santarelli, R. Gonnella, M. A. Romeo, G. D'Orazi, A. Faggioni, M. Cirone, Quercetin interrupts the positive feedback loop between STAT3 and IL-6, promotes autophagy, and reduces ROS, preventing EBV-driven B cell immortalization, Biomolecules 9 (2019).
[24] M. Krzyzowska, P. Baska, A. Grochowska, P. Orlowski, Z. Nowak, A. Winnicka, Fas/FasL pathway participates in resolution of mucosal inflammatory response early during HSV-2 infection, Immunobiology 219 (2014) 64–77.
[25] X. Wang, Z. Fu, Y. Chen, L. Liu, Fas expression is downregulated in gastric cancer, Mol. Med. Rep. 15 (2017) 627–634.
[26] S. Jangra, A. Bharti, W.Y. Lui, V. Chaudhary, M.G. Botelho, K.S. Yuen, D.Y. Jin, Suppression of JAK-STAT signaling by Epstein-Barr virus tegument protein BGLF2 through recruitment of SHP1 phosphatase and promotion of STAT2 degradation, J. Virol. 95 (2021) e0102721.
[27] M. Xing, W.F. Ooi, J. Tan, A. Qamra, P.H. Lee, Z. Li, C. Xu, N. Padmanabhan, J. Q. Lim, Y.A. Guo, X. Yao, M. Amit, L.M. Ng, T. Sheng, J. Wang, K.K. Huang, C. G. Anene-Nzelu, S.W.T. Ho, M. Ray, L. Ma, G. Fazzi, K.J. Lim, G.C. Wijaya, S. Zhang, T. Nandi, T. Yan, M.M. Chang, K. Das, Z.F.A. Isa, J. Wu, P.S.Y. Poon, Y. N. Lam, J.S. Lin, S.T. Tay, M.H. Lee, A.L.K. Tan, X. Ong, K. White, S.G. Rozen, M. Beer, R.S.Y. Foo, H.I. Grabsch, A.J. Skanderup, S. Li, B.T. Teh, P. Tan, Genomic and epigenomic EBF1 alterations modulate TERT expression in gastric cancer, J. Clin. Invest. 130 (2020) 3005–3020.
[28] Y. Li, J. Li, Z. Li, M. Wei, H. Zhao, M. Miyagishi, S. Wu, V. Kasim, Homeostasis imbalance of YY2 and YY1 promotes tumor growth by manipulating Ferroptosis, Adv Sci (Weinh) 9 (2022) e2104836.
[29] K. Yamazaki, Y. Masugi, K. Effendi, H. Tsujikawa, N. Hiraoka, M. Kitago, M. Shinoda, O. Itano, M. Tanabe, Y. Kitagawa, M. Sakamoto, Upregulated SMAD3 promotes epithelial-mesenchymal transition and predicts poor prognosis in pancreatic ductal adenocarcinoma, Lab. Invest. 94 (2014) 683–691.
[30] Q. Xiao, Y. Gan, Y. Li, L. Fan, J. Liu, P. Lu, J. Liu, A. Chen, G. Shu, G. Yin, MEF2A transcriptionally upregulates the expression of ZEB2 and CTNNB1 in colorectal cancer to promote tumor progression, Oncogene 40 (2021) 3364–3377.
[31] R. Neijts, S. Amin, C. van Rooijen, S. Tan, M.P. Creyghton, W. de Laat, J. Deschamps, Polarized regulatory landscape and Wnt responsiveness underlie Hox activation in embryos, Genes Dev. 30 (2016) 1937–1942.
[32] A. Hellman, A. Chess, Gene body-specific methylation on the active X chromosome, Science 315 (2007) 1141–1143.
[33] M.P. Ball, J.B. Li, Y. Gao, J.H. Lee, E.M. LeProust, I.H. Park, B. Xie, G.Q. Daley, G. M. Church, Targeted and genome-scale strategies reveal gene-body methylation signatures in human cells, Nat. Biotechnol. 27 (2009) 361–368.
[34] D. Aran, G. Toperoff, M. Rosenberg, A. Hellman, Replication timing-related and gene body-specific methylation of active human genes, Hum. Mol. Genet. 20 (2011) 670–680.
[35] L.J. Castro-Munoz, E.V. Ulloa, C. Sahlgren, M. Lizano, E. De La Cruz-Hernandez, A. Contreras-Paredes, Modulating epigenetic modifications for cancer therapy (review), Oncol. Rep. 49 (2023).
[36] V. Ebrahimi, A. Soleimanian, T. Ebrahimi, R. Azargun, P. Yazdani, S. Eyvazi, V. Tarhriz, Epigenetic modifications in gastric cancer: focus on DNA methylation, Gene 742 (2020) 144577.
[37] A. Goel, C.R. Boland, Epigenetics of colorectal cancer, Gastroenterology 143 (2012) 1442–1460 e1441.
[38] R. Hino, H. Uozaki, N. Murakami, T. Ushiku, A. Shinozaki, S. Ishikawa, T. Morikawa, T. Nakaya, T. Sakatani, K. Takada, M. Fukayama, Activation of DNA methyltransferase 1 by EBV latent membrane protein 2A leads to promoter hypermethylation of PTEN gene in gastric carcinoma, Cancer Res. 69 (2009) 2766–2774.
[39] K. Matsusaka, S. Funata, M. Fukuyo, Y. Seto, H. Aburatani, M. Fukayama, A. Kaneda, Epstein-Barr virus infection induces genome-wide de novo DNA methylation in non-neoplastic gastric epithelial cells, J. Pathol. 242 (2017) 391–399.
[40] M. Jain, S. Koren, K.H. Miga, J. Quick, A.C. Rand, T.A. Sasani, J.R. Tyson, A. D. Beggs, A.T. Dilthey, I.T. Fiddes, S. Malla, H. Marriott, T. Nieto, J. O'Grady, H. E. Olsen, B.S. Pedersen, A. Rhie, H. Richardson, A.R. Quinlan, T.P. Snutch, L. Tee, B. Paten, A.M. Phillippy, J.T. Simpson, N.J. Loman, M. Loose, Nanopore sequencing and assembly of a human genome with ultra-long reads, Nat. Biotechnol. 36 (2018) 338–345.
[41] K.H. Miga, S. Koren, A. Rhie, M.R. Vollger, A. Gershman, A. Bzikadze, S. Brooks, E. Howe, D. Porubsky, G.A. Logsdon, V.A. Schneider, T. Potapova, J. Wood, W. Chow, J. Armstrong, J. Fredrickson, E. Pak, K. Tigyi, M. Kremitzki, C. Markovic, V. Maduro, A. Dutra, G.G. Bouffard, A.M. Chang, N.F. Hansen, A.B. Wilfert, F. Thibaud-Nissen, A.D. Schmitt, J.M. Belton, S. Selvaraj, M.Y. Dennis, D.C. Soto, R. Sahasrabudhe, G. Kaya, J. Quick, N.J. Loman, N. Holmes, M. Loose, U. Surti, R. A. Risques, T.A. Graves Lindsay, R. Fulton, I. Hall, B. Paten, K. Howe, W. Timp, A. Young, J.C. Mullikin, P.A. Pevzner, J.L. Gerton, B.A. Sullivan, E.E. Eichler, A. M. Phillippy, Telomere-to-telomere assembly of a complete human X chromosome, Nature 585 (2020) 79–84.
[42] Y. Liu, W. Rosikiewicz, Z. Pan, N. Jillette, P. Wang, A. Taghbalout, J. Foox, C. Mason, M. Carroll, A. Cheng, S. Li, DNA methylation-calling tools for Oxford Nanopore sequencing: a survey and human epigenome-wide evaluation, Genome Biol. 22 (2021) 295.
[43] M.P. Hanley, M.A. Hahn, A.X. Li, X. Wu, J. Lin, J. Wang, A.H. Choi, Z. Ouyang, Y. Fong, G.P. Pfeifer, T.J. Devers, D.W. Rosenberg, Genome-wide DNA methylation profiling reveals cancer-associated changes within early colonic neoplasia, Oncogene 36 (2017) 5035–5044.
[44] M. Saito, J. Nishikawa, T. Okada, A. Morishige, K. Sakai, M. Nakamura, S. Kiyotoki, K. Hamabe, T. Okamoto, A. Oga, K. Sasaki, Y. Suehiro, Y. Hinoda, I. Sakaida, Role of DNA methylation in the development of Epstein-Barr virus-associated gastric carcinoma, J. Med. Virol. 85 (2013) 121–127.
[45] Q. Rosemarie, B. Sugden, Epstein-Barr virus: how its lytic phase contributes to oncogenesis, Microorganisms 8 (2020).
[46] G.K. Hong, M.L. Gulley, W.H. Feng, H.J. Delecluse, E. Holley-Guthrie, S.C. Kenney, Epstein-Barr virus lytic infection contributes to lymphoproliferative disease in a SCID mouse model, J. Virol. 79 (2005) 13993–14003.
[47] D. Zhang, S. Guo, S.J. Schrodi, Mechanisms of DNA methylation in virus-host interaction in hepatitis B infection: pathogenesis and Oncogenetic properties, Int. J. Mol. Sci. 22 (2021).
[48] J. Yang, Z. Liu, B. Zeng, G. Hu, R. Gan, Epstein-Barr virus-associated gastric cancer: a distinct subtype, Cancer Lett. 495 (2020) 191–199.
[49] G.N. Fiches, D. Zhou, W. Kong, A. Biswas, E.H. Ahmed, R.A. Baiocchi, J. Zhu, N. Santoso, Profiling of immune related genes silenced in EBV-positive gastric carcinoma identified novel restriction factors of human gammaherpesviruses, PLoS Pathog. 16 (2020) e1008778.
[50] J. Wu, Q. Tang, L. Yang, Y. Chen, F. Zheng, S.S. Hann, Interplay of DNA methyltransferase 1 and EZH2 through inactivation of Stat3 contributes to beta-elemene-inhibited growth of nasopharyngeal carcinoma cells, Sci. Rep. 7 (2017) 509.
[51] A. Barnicle, C. Seoighe, A. Golden, J.M. Greally, L.J. Egan, Differential DNA methylation patterns of homeobox genes in proximal and distal colon epithelial cells, Physiol. Genomics 48 (2016) 257–273.
[52] G. Manzo, Similarities between embryo development and Cancer process suggest new strategies for research and therapy of tumors: a new point of view, Front. Cell Dev. Biol. 7 (2019) 20.
[53] G.H. Kang, S. Lee, W.H. Kim, H.W. Lee, J.C. Kim, M.G. Rhyu, J.Y. Ro, Epstein-barr virus-positive gastric carcinoma demonstrates frequent aberrant methylation of multiple genes and constitutes CpG island methylator phenotype-positive gastric carcinoma, Am. J. Pathol. 160 (2002) 787–794.
[54] P. Pai, S. Sukumar, HOX genes and the NF-kappaB pathway: a convergence of developmental biology, inflammation and cancer biology, Biochim. Biophys. Acta Rev. Cancer 1874 (2020) 188450.
[55] I. Jridi, K. Cante-Barrett, K. Pike-Overzet, F.J.T. Staal, Inflammation and Wnt signaling: target for immunomodulatory therapy? Front. Cell Dev. Biol. 8 (2020) 615131.
[56] H. Clevers, Wnt/beta-catenin signaling in development and disease, Cell 127 (2006) 469–480.
[57] Y. Feng, T. Zhang, Y. Wang, M. Xie, X. Ji, X. Luo, W. Huang, L. Xia, Homeobox genes in cancers: from carcinogenesis to recent therapeutic intervention, Front. Oncol. 11 (2021) 770428.
[58] M.L. Golson, K.H. Kaestner, Fox transcription factors: from development to disease, Development 143 (2016) 4558–4570.
[59] L. Meurer, L. Ferdman, B. Belcher, T. Camarata, The SIX family of transcription factors: common themes integrating developmental and Cancer biology, Front. Cell Dev. Biol. 9 (2021) 707854.
[60] Y. Zhu, Y. Li, J.W. Jun Wei, X. Liu, The role of sox genes in lung morphogenesis and cancer, Int. J. Mol. Sci. 13 (2012) 15767–15783.
[61] M. Wachtel, B.W. Schafer, Unpeaceful roles of mutant PAX proteins in cancer, Semin. Cell Dev. Biol. 44 (2015) 126–134.
[62] R.A. Irizarry, C. Ladd-Acosta, B. Wen, Z. Wu, C. Montano, P. Onyango, H. Cui, K. Gabo, M. Rongione, M. Webster, H. Ji, J. Potash, S. Sabunciyan, A.P. Feinberg, The human colon cancer methylome shows similar hypo- and hypermethylation at conserved tissue-specific CpG island shores, Nat. Genet. 41 (2009) 178–186.
[63] S. Li, J. Zhang, S. Huang, X. He, Genome-wide analysis reveals that exon methylation facilitates its selective usage in the human transcriptome, Brief. Bioinform. 19 (2018) 754–764.
[64] A.Y. Lai, M. Fatemi, A. Dhasarathy, C. Malone, S.E. Sobol, C. Geigerman, D.L. Jaye, D. Mav, R. Shah, L. Li, P.A. Wade, DNA methylation prevents CTCF-mediated silencing of the oncogene BCL6 in B cell lymphomas, J. Exp. Med. 207 (2010) 1939–1950.
[65] I.K. Mann, R. Chatterjee, J. Zhao, X. He, M.T. Weirauch, T.R. Hughes, C. Vinson, CG methylated microarrays identify a novel methylated sequence bound by the CEBPB|ATF4 heterodimer that is active in vivo, Genome Res. 23 (2013) 988–997.
[66] A.J. Bannister, T. Kouzarides, Regulation of chromatin by histone modifications, Cell Res. 21 (2011) 381–395.
[67] Y. Li, X. Chen, C. Lu, The interplay between DNA and histone methylation: molecular mechanisms and disease implications, EMBO Rep. 22 (2021) e51803.
[68] T. Vaissiere, C. Sawan, Z. Herceg, Epigenetic interplay between histone modifications and DNA methylation in gene silencing, Mutat. Res. 659 (2008) 40–48.
[69] M. Janin, V. Davalos, M. Esteller, Cancer metastasis under the magnifying glass of epigenetics and epitranscriptomics, Cancer Metastasis Rev. 42 (2023) 1071–1112.
[70] M. Morlando, A. Fatica, Alteration of epigenetic regulation by long noncoding RNAs in Cancer, Int. J. Mol. Sci. 19 (2018).
[71] Q. Yao, Y. Chen, X. Zhou, The roles of microRNAs in epigenetic regulation, Curr. Opin. Chem. Biol. 51 (2019) 11–17.